Chapter 2

Replacing Fast Dynamics by Coupled OU Processes

Whereas Conditional Averaging is derived in terms of the ensemble dynamics (1.3), in this chapter our purpose is to think the approach over by examining the single system dynamics (1.1)&(1.2). In so doing, we will construct coupled fast-slow systems, where each approximates the fast dynamics in one of the (two) metastable sets. We thus obtain a stochastic process where the slow variable at each instant is coupled to one of two fast variables but where a stochastic switching process controls the switches from one fast variable to the other. With these preliminaries, we are in a position to apply well-known averaging techniques ([35, 28, 25, 15]) in order to arrive at a reduced model that describes the effective motion of the slow DOF in the limit $\epsilon \to 0$.

2.1 Guiding Remarks

The key assumption for the appropriateness of the limit model (1.18) is nicely illustrated in Figure 2.1 showing the course of the metastable decomposition in the full state space: We observe that the metastable decomposition do not depend on the slow variable x so that transitions between the subsets always happen along the direction of the y dynamics. This is exactly the situation where we can apply the conditionally averaged dynamics without doubt in order to reproduce the effective dynamics of the original system. Therefore, we will concentrate throughout the chapter on the situation that is illustrated in the picture.

We prescribe for the fast dynamics the simplest energy landscape exhibiting exactly two metastable subsets: For fixed x, the potential energy landscape in y will be given by a double-well potential. This allows us to consult the rich literature on the derivation of asymptotic formulas for transition rates between the potential wells. However, we must slightly modify

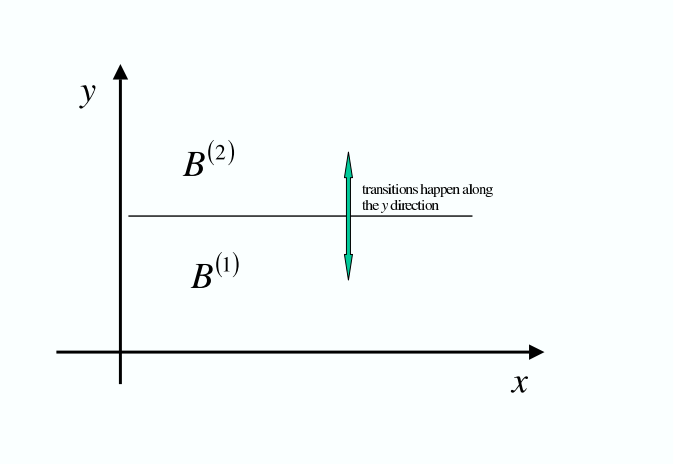

Figure 2.1: The boundary between the metastable decomposition does not depend on x which implies that transitions between $B^{(1)}$ and $B^{(2)}$ are solely caused by the y dynamics.

system (1.1)&(1.2), mainly for the following reason: Recall the scaling assumption (1.13) that justifies the need for Conditional Averaging. This is explicitly realized only if $\exp(-2V^x_{\text{bar}}/\sigma^2)$ scales like ϵ, which is achieved by either rescaling the potential barrier in an appropriate manner, or, as a second possibility, decreasing the noise intensity σ. We will choose the second way, for the approximation of the metastable fast dynamics by irreducible processes is justified for vanishing σ. This requires to uncouple the diffusion in the slow and the fast equation. Thus, we denote ς the noise amplitude in the fast equation and consider now

$$\dot{x}^\epsilon = -D_x V(x,y) + \sigma \dot{W}_1 \tag{2.1}$$

$$\dot{y}^\epsilon = -\frac{1}{\epsilon} D_y V(x,y) + \frac{\varsigma}{\sqrt{\epsilon}} \dot{W}_2, . \tag{2.2}$$

Here, we cannot easily write down an invariant density for the full dynamics, but for fixed slow variable x the invariant density on every fibre of the fast variables's state space will be given by

$$\mu_x(y) = \frac{1}{Z_x} \exp(-\frac{2}{\varsigma^2} V(x,y)), \quad Z_x = \int_{\mathbf{R}^n} \exp(-\frac{2}{\varsigma^2} V(x,y))\, \mathrm{d}y, \tag{2.3}$$

which is assumed to be the unique invariant density for every x.

The conditionally averaged dynamics (1.21) can equally well be obtained for differing noise in the slow (σ) and fast equation (ς), and the need for Conditional Averaging is now expressed by the scaling assumption

$$\bar{\tau}^\epsilon_x \simeq C(x)\, \epsilon \exp(\frac{2}{\varsigma^2} V^x_{\text{bar}}) = \text{ord}(1), \tag{2.4}$$

that depends on the diffusion in the fast equation. As we cannot assume that the full dynamics admit a (unique) invariant probability density (respectively, we cannot write it down as a Gibbs measure), the asymptotic procedure as is done in [43] has to be modified wrt. the Fokker-Planck equation in the unweighted function space $L^2(\mathbf{R}^2)$ (for $x, y \in \mathbf{R}$). However, for fixed slow variable x the fast dynamics (2.2) admit the (assumed unique) invariant density μ_x as defined in (2.3), and, consequently, the conditionally averaged dynamics are given by (1.21) as well[1]. However, to obtain the corresponding averaged potentials $\overline{V}^{(1)}$ and $\overline{V}^{(2)}$, we have to replace the inverse temperature β in (1.22) by $2/\varsigma^2$.

We conclude the introductory comments by briefly discussing the questions arising from (1.18) that are addressed by the approach 'Replacing fast dynamics by coupled OU processes'.

Questions Arising from Conditional Averaging

The limit equation (1.21) is formally derived by exploiting the scaling assumption (1.15) together with the approximation of the second eigenfunction $u_1(x, \cdot)$ by step functions that are constant on the metastable subsets $B_x^{(1)}$ and $B_x^{(2)}$. Aiming at a numerical integration of the system immediately poses the question of how to derive the metastable decomposition. In the context of numerical schemes designed to recover metastable sets from the computation of eigenfunctions, there is a considerable interest in the knowledge of the eigenfunction $u_1(x, \cdot)$ that becomes an excellent approximation of the indicator functions of the metastable sets. Relating the structure of the eigenfunction according to (1.14) to the potential energy landscape yields the result that the eigenfunction will drop sharply at the saddle point that separates two potential wells. Following [43], we define the almost invariant subsets by the zero of the eigenfunction $u_1(x, \cdot)$:

$$B_x^{(1)} = \{y \in \mathbf{R} \mid u_1(x, y) < 0\}, \qquad B_x^{(2)} = \{y \in \mathbf{R} \mid u_1(x, y) > 0\}. \quad (2.5)$$

The problem of finding the zero z in the asymptotic limit $\sigma \to 0$ has been a subject of controversy in several articles. In [20, 8] it is the belief that

[1]For ease of presentation we omit the procedure, other than remarking that it starts from the dynamics

$$\partial_t p^\epsilon = (\frac{1}{\epsilon}\mathcal{A}_x + \mathcal{A}_y)p^\epsilon,$$

where p^ϵ is the physical probability density and $\mathcal{A}_x$, $\mathcal{A}_y$ denote the generators for the fast and the slow dynamics, respectively. For fixed slow variable x we can switch to the generator $\mathcal{L}_x : L^2(\mu_x) \to L^2(\mu_x)$ that is related to $\mathcal{A}_x$ by

$$p^\epsilon(t, x, y) = d^\epsilon(t, x, y)\,\mu_x(y) \quad \Longrightarrow \quad \mathcal{A}_x p^\epsilon(t, x, \cdot) = \mu_x\,\mathcal{L}_x d^\epsilon(t, x, \cdot).$$

The decomposition (1.16) can be easily applied to $\mathcal{A}_x$, with corresponding modifications to the steps between (1.16) and (1.18).

the zero is generally not in the neighbourhood of the saddle point but much closer to the minimum in the deep well of the potential. However, using the results in [36] suggests to rather approximate the zero by the saddle point. The difficulty of finding the correct decomposition concerns not only the restricted probability density (1.20) that is used to obtain the averaged potentials $\overline{V}^{(i)}$, $i = 1, 2$ in (1.22), but also the rate matrix $\mathcal{Q}_x$. Therefore, to overcome the problem, we must carefully examine the entries of $\mathcal{Q}_x$. This immediately brings us to the decisive question of how to establish a relation between the entries of $\mathcal{Q}_x$ and the exit rates/times from metastable subsets in the fast DOF. In the Wentzell-Freidlin setting of large deviation theory ([15]), relations between the dominant spectrum of the generator $\mathcal{L}_x$ and the potential energy landscape are studied. It can be shown that in the limit of vanishing noise amplitude σ, the dominant eigenvalues are related to the inverse mean transition times between two potential wells being separated by an energy barrier. Consequently, we have to study especially the following questions:

(Q1) Does the matrix $\mathcal{Q}_x$ actually capture the transition behaviour between the metastable states in the full dynamics description? What exactly is the relation between the dominant eigenvalue λ_1 and the expected inter-well transition rates for some given potential energy landscape?

(Q2) How should the metastable decomposition then be defined?

Based on observations from studying (Q1), we hope to understand how (2.4) is connected to the scaling assumption (1.15) that is explicitly required for the asymptotic procedure performed to obtain the conditionally averaged dynamics. According to (2.4), the metastable transitions can only be frozen on an order unity time scale, if $2V^x_{\mathrm{bar}}/\varsigma^2$ scales as $-\ln\epsilon$. This brings us to the last question[2]:

(Q3) Assuming that the potential energy barrier does not change, how do we have to couple ς to ϵ such that the scaling assumption (2.4) is fulfilled?

2.2 Theory

Subsequently we study the SDE (2.1)&(2.2), where the following basic assumptions about the potential $V = V(x, y)$ are made:

Assumption 2.2.1 *(i.)* $V \in \mathcal{C}^\infty(\mathbf{R}^{m+1})$;

[2]The question of how to rescale the potential energy barrier will be considered in Chapter 3.

(ii.) $V(x,\cdot)$ *is a double-well potential for all* $x \in \mathbf{R}^m$ *with two local minima at* $y = m^{(1)}, m^{(2)}$ *and one local maximum at* $y = y_0$ *with* $m^{(1)} < y_0 < m^{(2)}$*; to point out the dependence on* x *we will also write* $m^{(i)}(x)$, $i = 1,2$ *and* $y_0(x)$*, respectively;*

(iii.) the position of the saddle point does not depend on x*, without loss of generality we may assume* $y_0(x) = 0$ *for every* x*;*

(iv.) the extrema are non-degenerate, i.e., for $i = 1,2$

$$D_{yy}V(x, m^{(i)}) = \omega^{(i)}(x) > 0, \qquad D_{yy}V(x, y_0) = -\omega_0(x) < 0.$$

Therefore, for fixed x, the particle spends a 'long time' in one basin (=potential well), then quickly undergoes a transition into the other basin, in which it spends another 'long time', and so on. The condition $y_0(x) = 0$ implies that for every $x \in \mathbf{R}^m$ the locations of the two basins do not depend on x such that the natural decomposition of the entire state space into metastable subsets is simply given by $B^{(1)} \cup B^{(2)}$, where[3]

$$B^{(1)} = \{(x,y) \in \mathbf{R}^{m+1} \mid y < 0\}, \quad B^{(2)} = \{(x,y) \in \mathbf{R}^{m+1} \mid y > 0\}. \tag{2.6}$$

The double-well potentials may serve as toy models mimicking a larger system whose potential energy surface presents several basins corresponding to metastable states. The design of $V(x,\cdot)$ already suggests that an averaging procedure should incorporate metastabilities in the fast dynamics that are induced by the double-well structure.

We give a short illustration of the theory develop throughout Section 2.2. To help orient the reader, we present the different steps in Figure 2.2. If the noise level in the fast equation is small, the diffusion sample paths are located near the local minima of the potential wells, and transitions between the two potential wells can be considered as rare events. Then, the diffusion can be decomposed into two *almost* irreducible subprocesses

$$\begin{aligned} \big(x^\epsilon(t), y^\epsilon_{(1)}(t)\big) &= \big(x^\epsilon(t), y^\epsilon(t)\big)\, \mathbf{1}_{B^{(1)}}\big(x^\epsilon(t), y^\epsilon(t)\big), \\ \big(x^\epsilon(t), y^\epsilon_{(2)}(t)\big) &= \big(x^\epsilon(t), y^\epsilon(t)\big)\, \mathbf{1}_{B^{(2)}}\big(x^\epsilon(t), y^\epsilon(t)\big), \end{aligned}$$

and a two-state Markov chain $I(t,x)$ mimicking the transitions between $B^{(1)}$ and $B^{(2)}$ which happen along the y dynamics and thus depend on the position of the slow one. In Section 2.2.1 we approximate for fixed x each of the subprocesses $y^\epsilon_{(i)}$, $i = 1,2$ by an appropriately chosen Ornstein-Uhlenbeck process (OU process), which is given in (2.10). As a consequence, we obtain two irreducible processes $y^\epsilon_{\mathrm{OU}(1)}$ and $y^\epsilon_{\mathrm{OU}(2)}$ evolving independently of each

[3] In [43], the metastable decomposition for fixed x is defined by the zero z of the second eigenfunction $u_1(x,\cdot)$ of the fast dynamics generator. We show in Section 2.2.6 that the zero z of $u_1(x,\cdot)$ actually is approximated by the saddle point of the potential $V(x,\cdot)$.

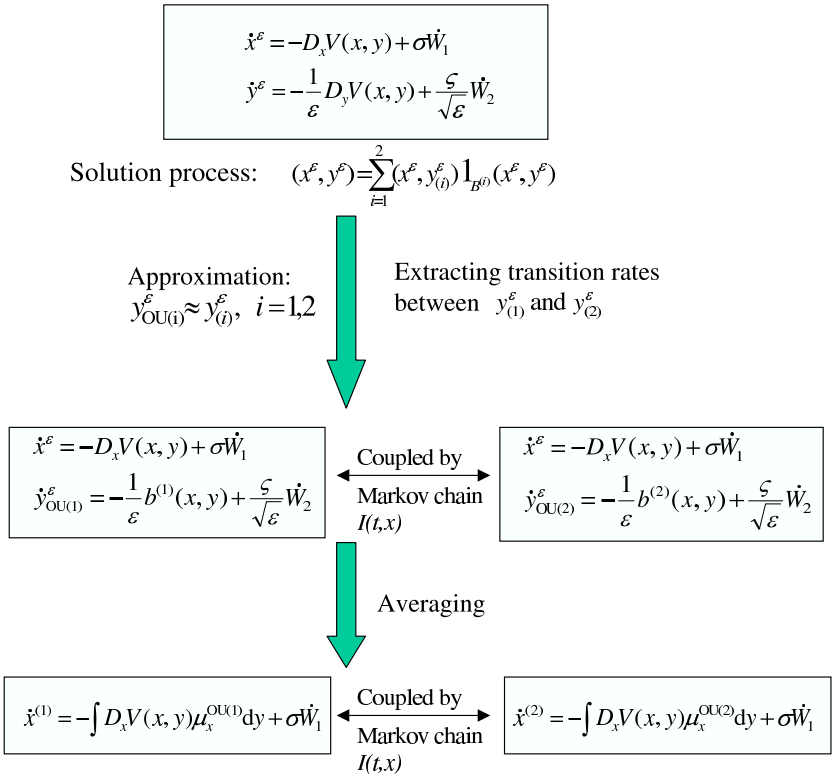

Figure 2.2: Illustration of the approach 'Replacing metastable fast dynamics by coupled OU processes'.

other. The result can be mathematically justified for vanishing diffusion in the fast equation (2.2). To quantify the rates at which the process moves between the two varying OU processes for fixed x, we consider the distribution of the first exit times from the metastable subsets of the fast dynamics in Section 2.2.2. For vanishing diffusion term in the fast equation we obtain asymptotics for the expected exit times that are used to parametrize the Markov switching process $I(t,x)$ that regulates the transitions between the OU processes. To this end, we define the exchange rates between the metastable states of the fast dynamics as the inverse of the expected exit times for fixed x. In Section 2.2.3 we summarize the achieved results by incorporating the slow variable dynamics in x. The approximated system is given in (2.31)&(2.32), where the Markov chain $I(t,x)$ is generated by the rate matrix $\mathcal{Q}_x$ whose entries are explicitly given in (2.30).

In Section 2.2.4 we use the system with coupled OU processes as the basis to obtain an appropriate averaged model. The reduced model then describes the effective motion in the slow DOF. We present the asymptotic strategy that is based on a perturbation expansion in the smallness parameter ϵ of the partial differential equation associated with the stochastic model equations. In so doing, we start from the Fokker-Planck equation (2.38). The essential point in the averaging strategy is that the fast dynamics now are given by two (respectively N) irreducible processes (replacing the *almost* irreducible motion in the double-well potential). The averaged model in (2.47) is then obtained by projecting the full dynamics onto the invariant density $\mu_x^{\mathrm{OU}(i)}$ of the OU process $y^\epsilon_{\mathrm{OU}(i)}$ for $i \in \{1, 2, ..., N\}$, where the evolution of the Markov chain $I(t, x)$ controls the switches on the state space $\mathbf{S} = \{1, 2, ..., N\}$.

2.2.1 Approximation of Fast Dynamics by OU Processes

The present section builds upon the assumed double-well structure of the potential energy surface $V(x, \cdot)$ for fixed x, see Assumption 2.2.1. For simplicity, we assume the function $V(x, \cdot)$ to be a fourth-degree polynomial. For small noise intensity ς, the process y^ϵ corresponding to the Smoluchowski equation (2.2) for fixed x is almost decomposable[4] into two subprocesses $y^\epsilon_{(1)}$, $y^\epsilon_{(2)}$, each attracted to a minimum $m^{(i)}(x)$, $i = 1, 2$ of the function $V(x, \cdot)$.

Thus, we consider the fast motion $y^\epsilon_x(t)$ for fixed slow variables $x \in \mathbf{R}^m$:

$$\dot{y}^\epsilon_x \;=\; -\frac{1}{\epsilon} D_y V(x, y^\epsilon_x) \;+\; \frac{\varsigma}{\sqrt{\epsilon}}\, \dot{W}_2, \tag{2.7}$$

and distinguish between the two different regions of attraction $O_x^{(1)}$ and $O_x^{(2)}$ where $O_x^{(i)}$ is an open subset of $B_x^{(i)}$ with $m^{(i)}(x)$ in its interior. The subsets $B_x^{(1)}$ and $B_x^{(2)}$ are defined by the potential energy barrier:

$$B_x^{(1)} \;=\; \{y \in \mathbf{R} : y \,<\, y_0(x)\}, \quad \text{and} \quad B_x^{(2)} \;=\; \{y : y \,>\, y_0(x)\}, \tag{2.8}$$

with $y_0(x) = 0$ denoting the saddle point of the potential $V(x, \cdot)$. For ς small we can almost decouple the process y^ϵ into two subprocesses $y^\epsilon_{(1)}(t) \in O_x^{(1)}$ and $y^\epsilon_{(2)}(t) \in O_x^{(2)}$. For vanishing noise intensity ς, in each of the subsets $O_x^{(i)}$ the fast diffusion will consist of small fluctuations around the potential minima $m^{(1)}(x)$ and $m^{(2)}(x)$, respectively. The drift term in (2.2) can now be expanded in a Taylor series with respect to y. Taylor-expansion of $D_y V(x, \cdot)$ around $m^{(i)}(x)$, $i = 1, 2$ gives

$$D_y V(x, y) \;\;=\;\; D_{yy} V(x, m^{(i)}(x)) \cdot (y - m^{(i)}(x)) + \mathcal{O}(|y - m^{(i)}(x)|^2), \tag{2.9}$$

[4] The notion 'almost decomposable' is used to indicate that we cannot consider the two 'subprocesses' as evolving independently of each other. Instead we have to wait a finite time only until the dynamics change from $y^\epsilon_{(i)}$ to $y^\epsilon_{(j)}$ for $i \neq j$.

where we have used $D_y V(x, m^{(i)}(x)) = 0$. For y sufficiently close to $m^{(i)}(x)$, this provides us with an approximation of the SDE (2.7):

$$\dot{y}^\epsilon_{\mathrm{OU}(i)} \;=\; -\frac{1}{\epsilon}\omega^{(i)}(x)\cdot\big(y^\epsilon_{\mathrm{OU}(i)} - m^{(i)}(x)\big) \;+\; \frac{\varsigma}{\sqrt{\epsilon}}\,\dot{W}_2, \tag{2.10}$$

with $\omega^{(i)}$, $i = 1, 2$ denoting the curvature of $V(x, \cdot)$ in $m^{(i)}(x)$

$$\omega^{(i)}(x) \;=\; D_{yy}V(x, m^{(i)}(x)).$$

The solution of the stochastic differential equation (2.10) is known as a process of Ornstein-Uhlenbeck type, or OU process for short. To distinguish it from the 'decoupled' processes $y^\epsilon_{(i)}$, $i = 1, 2$ that originate from (2.7) we denote it $y^\epsilon_{\mathrm{OU}(i)}$ for $i = 1, 2$. We omit the index for the fixed variable x.

The quality of the approximation will depend on how close the original motion stays in the vicinity of the minima $m^{(i)}(x)$, $i = 1, 2$. Consequently, we expect the approximation error decreases for vanishing ς. This can be made more precise by applying the small noise expansion method for stochastic differential equations. Since noise is often small, this is a method of wide practical application. The basic assumption of asymptotically expanding the solution process $y^\epsilon_{(i)}$ for $i = 1, 2$ into powers of the noise intensity ς leads to a reduction of the equation (2.7) into a sequence of time-dependent OU processes. Mostly the first order is quite adequate and amounts to a linearisation of the original equation about the deterministic solution. The reader may refer to [16], where it is shown that the procedure up to first order yields pathwise convergence in the asymptotic limit $\varsigma \to 0$, more precise,

$$\mathbf{E}\,|y^\epsilon_{(i)}(t) \;-\; y^\epsilon_{\mathrm{OU}(i)}(t)| \;=\; \mathcal{O}(\varsigma^2), \qquad\qquad i = 1, 2.$$

Comparison of Stationary Densities

The stationary solution is obtained by letting $t \to \infty$. As the OU process (2.10) is ergodic, the stationary density $\mu_x^{\mathrm{OU}(i)}$ is simply given by the Gaussian with mean $m^{(i)}(x)$ and variance $\varsigma^2/(2\omega^{(i)}(x))$. If we denote the invariant density corresponding to equation (2.7) by μ_x, it is sensible to compare $\mu_x^{\mathrm{OU}(i)}$, $i = 1, 2$ with $\mu_x^{(i)}$ where

$$\mu_x^{(i)}(y) \;\;=\;\; \frac{1}{\mu_x(B_x^{(i)})}\,\mu_x(y)\,\mathbf{1}_{B_x^{(i)}}(y), \qquad i = 1, 2. \tag{2.11}$$

Our goal is to show that $\mu_x^{\mathrm{OU}(i)}$ comes arbitrarily close to $\mu_x^{(i)}$ in $L^1(\mathbf{R})$ for vanishing diffusion term ς. There is no loss of generality in assuming $V(x, m^{(i)}(x)) = 0$ for fixed $i \in \{1, 2\}$. Then, the densities can be written

$$\begin{aligned}
\mu_x^{\mathrm{OU}(i)}(y) \;\;&=\;\; \frac{1}{Z_x^{\mathrm{OU}(i)}}\,\exp\Big(-\frac{\omega^{(i)}(x)}{\varsigma^2}\big(y - m^{(i)}(x)\big)^2\Big),\\
\mu_x^{(i)}(y) \;\;&=\;\; \frac{1}{Z_x^{(i)}}\,\exp\big(-\frac{2}{\varsigma^2}V(x,y)\big)\,\mathbf{1}_{B_x^{(i)}}(y),
\end{aligned}$$

with $Z_x^{\mathrm{OU}(i)}$ and $Z_x^{(i)}$ denoting appropriate normalization constants that depend on ς. We now use standard asymptotics that will allow to evaluate $\|\mu_x^{(i)} - \mu_x^{\mathrm{OU}(i)}\|_{L^1}$ in the asymptotic limit $\varsigma \to 0$. We first examine the normalization constants: $Z_x^{\mathrm{OU}(i)}$ is given explicitly, whereas for $Z_x^{(i)}$ we use the method of Laplace in order to obtain the main contribution to the integral in the asymptotic limit $\varsigma \to 0$. This yields

$$\begin{aligned} Z_x^{\mathrm{OU}(i)} &= \int \exp\Big(-\frac{\omega^{(i)}(x)}{\varsigma^2}\big(y - m^{(i)}(x)\big)^2\Big)\,\mathrm{d}y \;=\; \varsigma\sqrt{\frac{\pi}{\omega^{(i)}(x)}}, \\ Z_x^{(i)} &= \varsigma\sqrt{\frac{\pi}{\omega^{(i)}(x)}}(1+\mathcal{O}(\varsigma)) \;\doteq\; \varsigma\sqrt{\frac{\pi}{\omega^{(i)}(x)}}. \end{aligned}$$

For an explanation of Laplace's method we refer to Appendix D. In order to obtain the asymptotics of $\|\mu_x^{\mathrm{OU}(i)} - \mu_x^{(i)}\|_{L^1}$ in the limit $\varsigma \to 0$, we decompose the integral according to

$$\begin{aligned} \int_{-\infty}^{\infty} |\mu_x^{\mathrm{OU}(i)}(y) - \mu_x^{(i)}(y)|\mathrm{d}y &= \int_{-\infty}^{m^{(i)}(x)-C\varsigma} |\mu_x^{\mathrm{OU}(i)}(y) - \mu_x^{(i)}(y)|\mathrm{d}y \\ &+ \int_{m^{(i)}(x)-C\varsigma}^{m^{(i)}(x)+C\varsigma} |\mu_x^{\mathrm{OU}(i)}(y) - \mu_x^{(i)}(y)|\mathrm{d}y \\ &+ \int_{m^{(i)}(x)+C\varsigma}^{\infty} |\mu_x^{\mathrm{OU}(i)}(y) - \mu_x^{(i)}(y)|\mathrm{d}y, \end{aligned} \tag{2.12}$$

with $C > 0$ denoting a positive constant. We first compute the middle term on the RHS of (2.12). To this end, we use Taylor-expansion of $V(x,\cdot)$ around the minimum $m^{(i)}(x)$, which yields

$$V(x,y) \;=\; \frac{1}{2}\omega^{(i)}(x)\big(y - m^{(i)}(x)\big)^2 \,+\, \mathcal{O}((y - m^{(i)}(x))^3).$$

Thus, we get

$$\begin{aligned} &\int_{m^{(i)}(x)-C\varsigma}^{m^{(i)}(x)+C\varsigma} |\mu_x^{\mathrm{OU}(i)}(y) - \mu_x^{(i)}(y)|\,\mathrm{d}y \\ &= \int_{m^{(i)}(x)-C\varsigma}^{m^{(i)}(x)+C\varsigma} e^{-\frac{\omega^{(i)}(x)}{\varsigma^2}(y-m^{(i)}(x))^2}\left|\frac{1}{Z_x^{\mathrm{OU}(i)}} - \frac{e^{-\frac{2}{\varsigma^2}\mathcal{O}((y-m^{(i)}(x))^3)}}{Z_x^{(i)}}\mathbf{1}_{B_x^{(i)}}\right|\mathrm{d}y \\ &= \varsigma\int_{-C}^{C} e^{-\omega^{(i)}(x)y^2}\left|\frac{1}{Z_x^{\mathrm{OU}(i)}} - \frac{e^{-\frac{2}{\varsigma^2}\mathcal{O}(\varsigma^3 y^3)}}{Z_x^{(i)}}\mathbf{1}_{B_x^{(i)}}\big(m^{(i)}(x)+\varsigma y\big)\right|\mathrm{d}y. \end{aligned}$$

For fixed $C > 0$ we clearly observe that the correction term $e^{-\frac{2}{\varsigma^2}\mathcal{O}((\varsigma y)^3)}$ uniformly converges to 1 for $y \in [-C, C]$. Together with

$$\frac{\varsigma}{Z_x^{(i)}} \;\doteq\; \frac{\varsigma}{Z_x^{\mathrm{OU}(i)}} \;=\; \sqrt{\frac{\omega^{(i)}(x)}{\pi}},$$

we obtain in the limit $\varsigma \to 0$

$$\int_{m^{(i)}(x)-C\varsigma}^{m^{(i)}(x)+C\varsigma} |\mu_x^{\mathrm{OU}(i)}(y) - \mu_x^{(i)}(y)| \, \mathrm{d}y \quad \doteq \quad 0.$$

For the first term on the RHS of (2.12) we simply show that we always find a $C > 0$, such that the values of the integrals

$$\int_{-\infty}^{m^{(i)}(x)-C\varsigma} \mu_x^{(i)}(y) \, \mathrm{d}y, \qquad \int_{-\infty}^{m^{(i)}(x)-C\varsigma} \mu_x^{\mathrm{OU}(i)}(y) \, \mathrm{d}y, \tag{2.13}$$

come arbitrarily close to 0. To estimate the first expression we use

$$V(x,y) \quad = \quad (m^{(i)}(x) - y)^2 \, \mathrm{P}_2(x,y),$$

with $\mathrm{P}_2(x,y)$ being a polynomial in y of degree 2 and

$$\lim_{\varsigma \to 0} \mathrm{P}_2(x, m^{(i)}(x) + \varsigma y) \; = \; \mathrm{P}_2(x, m^{(i)}(x)) \; > \; 0$$

pointwise for every y. Therefore, we obtain in the asymptotic limit $\varsigma \to 0$

$$\begin{aligned} \int_{-\infty}^{m^{(i)}(x)-C\varsigma} \mu_x^{(i)}(y) \, \mathrm{d}y \quad &= \quad \frac{\varsigma}{Z_x^{(i)}} \int_{-\infty}^{-C} e^{-2y^2 \, \mathrm{P}_2(x, m^{(i)} + \varsigma y)} \mathrm{d}y \\ &\doteq \quad \sqrt{\frac{\omega^{(i)}(x)}{\pi}} \int_{-\infty}^{-C} e^{-2y^2 \mathrm{P}_2(x, m^{(i)}(x))} \, \mathrm{d}y. \end{aligned}$$

This shows that we can always find a $C > 0$ such that the value of the integral is arbitrarily close to 0. The second expression in (2.13) is evaluated analogously. The same estimates can be applied to the third term on the RHS of (2.12), such that altogether we end up with

$$\lim_{\varsigma \to 0} (\mu_x^{(i)} - \mu_x^{\mathrm{OU}(i)}) \; = \; 0, \qquad \text{in } L^1(\mathbf{R}).$$

Note that we do not get convergence in L^∞.

2.2.2 Construction of the Transition Rate Matrix

In Section 2.2.1 we considered the fast dynamics (2.7) restricted to a single metastable set and approximated it by a simple OU process mimicking the rapid mixing in each of these subsets prior to exiting. To address the question of the essential dynamical structure in the entire (fast) state space we consider the statistics of the exit times from the metastable sets and approximate the transition events of the diffusion by jump times of an associated continuous-time, finite state-space Markov chain (the double-well potential implies a two-state Markov chain).

If we know the location of the metastable basins, the mean exit times can be easily estimated from MD simulations. These data can then be used to construct a transition rate matrix $\mathcal{Q}$ that generates stochastic matrices $\exp(t\mathcal{Q})$ for all times $t > 0$ allowing for a pathwise simulation of the transitions between the metastable components. However, the computational effort of estimating the expected exit times can be avoided by resorting to the rich literature on the derivation of asymptotic formulas for the jump rates that are strongly connected to the dominant spectrum of the corresponding generator, see e.g. [36, 8, 7, 2].

We present formulas for the expected inter-well transition times in the asymptotic limit $\varsigma \to 0$, which are given for $\epsilon = 1$ in (2.15)&(2.16). Then we use the precise estimates to construct the transition rate matrix $\mathcal{Q}$, see (2.17). In addition, we link the transition rates to the dominant spectrum of the corresponding generator, which reveals an equivalent representation of $\mathcal{Q}$ in (2.20). We illustrate the validity of the asymptotic formulas through results from appropriate numerical experiments. Finally, we incorporate the smallness parameter ϵ and address the question of how to freeze the transitions on a time scale that is independent of ϵ. This can explicitly only realized if ϵ scales like $\exp(-(2/\varsigma^2)\Delta V)$ with ΔV denoting the potential barrier that has to be crossed. Thus, fixing the potential barrier height, will result in a logarithmic scaling of ς.

Let us fix the notation that will be used throughout Section 2.2.2. To simplify notation we will omit the index x in $V(x,\cdot)$ and assume that $V(y)$ is a strictly positive one-dimensional asymmetric double-well potential with non-degenerate extrema, compare Assumption 2.2.1. We consider the corresponding Smoluchowski equation

$$\dot{y} \;=\; -D_y V(y) \,+\, \varsigma\, \dot{W}, \tag{2.14}$$

with stationary density $\mu = \mu(y)$:

$$\mu(y) \,=\, \frac{1}{Z} \exp\big(-\frac{2}{\varsigma^2} V(y)\big), \qquad Z \,=\, \int \exp\big(-\frac{2}{\varsigma^2} V(y)\big)\, \mathrm{d}y.$$

We identify the left and right wells by m_1, m_2, and the local maximum by y_0. In order to prevent a possible mix-up with the corresponding notations in the two-dimensional case $V = V(x,y)$, we prefer to use the index $i \in \{1,2\}$ without brackets, and whenever possible we put it at the bottom of the parameters. The left and right potential barriers are denoted $V_{\mathrm{bar}}^1 = V(y_0) - V(m_1)$, $V_{\mathrm{bar}}^2 = V(y_0) - V(m_2)$, and let

$$V_{\mathrm{bar}} \,=\, \min\{V_{\mathrm{bar}}^1, V_{\mathrm{bar}}^2\}$$

denote the minimal potential barrier. Without loss of generality we assume that the saddle point is $y_0 = 0$ ($\Rightarrow\ m_1 \in \mathbf{R}^-$, $m_2 \in \mathbf{R}^+$), and $V_{\mathrm{bar}} = V_{\mathrm{bar}}^1$, i.e., the shallow well is at the left side and the deep well at the right. An

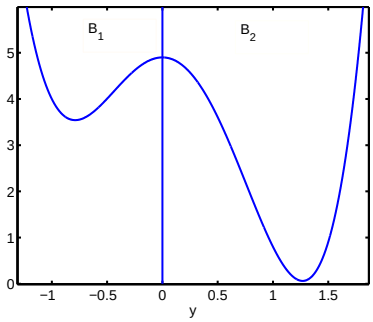

Figure 2.3: Asymmetric double-well potential with metastable decomposition $\mathbf{R} = B_1 \cup B_2$.

illustration of the potential thus defined is shown in Figure 2.3. The picture shows the natural decomposition of the state space into the metastable subsets B_1 and B_2:

$$B_1 = \{y \in \mathbf{R} \,|\, y < y_0 = 0\}, \qquad B_2 = \{y \in \mathbf{R} \,|\, y > y_0 = 0\}.$$

Metastability and Exit Times

Once having identified the metastable subsets, the question remains how to compute the transition rates between them. The problem is attacked by using some results concerning the expected exit time from a subset D of the state space containing (exactly) one local minimum of the potential in its interior (and some neighbourhood of the saddle point the process has to cross). Whenever the diffusion term is small, the system will be with overwhelming probability near the local minimum and far from ∂D. Nevertheless, the trajectories of the process will leave D with probability one. We are interested in the asymptotic behaviour of the expected transition times from one metastable subset of the system to the other. There is a variety of works on this subject done by probabilists starting at least from Freidlin & Wentzell, see [15]. The first papers only gave the asymptotic behaviour of the logarithm of expected exit times. The main contribution of [36, 8, 7] was to determine the main term in the prefactor. We will refer to [36] in the following, where the prefactor is established for a double-well potential.

If the diffusion in (2.14) is small, the diffusion sample paths of the process are located near the local minima of the potential wells, m_1 and m_2. If we consider the new discrete-space process on $\{m_1, m_2\}$, it assigns information about the inter-well dynamics of the diffusion. The intra-well small fluctuations of the diffusion in the potential minima are now filtered out. For small noise intensity ς, transitions between the potential wells occur at Kramers' time that is given up to exponential order by $\exp((2/\varsigma^2)\Delta V)$, where ΔV is the potential barrier that the process must cross to reach the other potential well. Let us render the result more precisely introducing the

first exit time of the Markov process $y(t)$ from D started at $y(0) = y$

$$\tau_D(y) \,=\, \inf\left\{t \in \mathbf{R}^+ : \int_0^t \mathbf{1}_D(y(s))\,\mathrm{d}s > 0,\, y(0) = y\right\}.$$

This measures only exits that happen for some non-null time interval and depends on the realization of the Markov process.

We are interested in the transition times between the metastable subsets B_1 and B_2. If the noise intensity does not vanish, they are not identical to the exit times τ_{B_i}, $i = 1, 2$. Instead we have to modify the metastable subsets slightly such that a (small) neighbourhood around the saddle point is included, i.e., we consider $B_1 + \delta = (-\infty, \delta)$ and $B_2 - \delta = (-\delta, \infty)$ instead with $\delta > 0$ being a small parameter. We assume that $O_1 \subset B_1$ and $O_2 \subset B_2$ are some regions of attraction (excluding a neighbourhood around the saddle point and including the potential minima, that is, $y_i \in O_i$ for $i = 1, 2$). Then, it is natural that the first exit times from $B_1 + \delta$ and $B_2 - \delta$ are basically independent for all starting points $y \in O_1$ and $y \in O_2$, respectively. This enables us to assign the expected exit times from $B_1 + \delta$ and $B_2 - \delta$ to the entire subsets O_1 and O_2 rather than to single points. An application of [15] or [20, 40] yields the following asymptotes as $\varsigma \to 0$:

(i) for $y \in O_1$ we have $\lim_{\varsigma\to 0} \varsigma^2 \log \mathbf{E}_y[\tau_{B_1+\delta}] \,=\, 2\, V^1_{\mathrm{bar}}$;

(ii.) for $y \in O_2$ we have $\lim_{\varsigma\to 0} \varsigma^2 \log \mathbf{E}_y[\tau_{B_2-\delta}] \,=\, 2\, V^2_{\mathrm{bar}}$.

However, for our purpose we need a result from Pavlyukevich in [36] that will give coincidence of the reducing Markov chain up to the sub-exponential prefactors which do not appear in the large deviations' statements. These are expressed in terms of the curvature of the potential in the saddle point and the minima:

$$D_{yy}V(m_1) \,=\, \omega_1, \quad D_{yy}V(m_2) \,=\, \omega_2, \quad D_{yy}V(y_0 = 0) \,=\, -\omega_0.$$

Now, the following result is obtained: Suppose that ς is sufficiently small and denote the expected transition time from B_i to B_j with $i \neq j$ by $\mathcal{T}_{i\to j}$, then $\mathcal{T}_{1\to 2}$ and $\mathcal{T}_{2\to 1}$ are well approximated by

$$\mathcal{T}_{1\to 2} \,=\, \mathbf{E}_{y\in O_1}[\tau_{B_1+\delta}] \;\simeq\; \frac{2\pi}{\sqrt{w_1\,\omega_0}}\,\exp(\frac{2}{\varsigma^2}V^1_{\mathrm{bar}}), \tag{2.15}$$

$$\mathcal{T}_{2\to 1} \,=\, \mathbf{E}_{y\in O_2}[\tau_{B_2-\delta}] \;\simeq\; \frac{2\pi}{\sqrt{w_2\,\omega_0}}\,\exp(\frac{2}{\varsigma^2}V^2_{\mathrm{bar}}). \tag{2.16}$$

In [36], the result is obtained in terms of the lowest eigenvalue $\neq 0$ of the associated infinitesimal generator, which corresponds (apart from suitable weights) to the inverse of the expected diffusion exit times. We discuss the connection in the next subsection.

Remark 2.2.2 *We emphasize again that in the following we will speak of (metastable) transition times between B_1 and B_2 or* metastable *exit times instead of exit times from B_i, $i = 1, 2$, for the precise asymptotic estimates in (2.15)&(2.16) are given for the mean values of the first exit times from $B_1 + \delta$ and $B_2 - \delta$ with $\delta > 0$. In Table 2.1 (in this section) it actually becomes apparent that the precise choice of the parameter δ is not important, and that the transition problem for B_1 to B_2 is virtually equivalent to considering the escape from a suitably chosen neighbourhood of m_1, provided this neighbourhood contains in its interior the relevant saddle point y_0 connecting m_1 and m_2. Therefore, we could equivalently define the first hitting time of a small (open) ball O_2 around m_2 (excluding a neighbourhood of the saddle point) for the process $y(t)$ starting in a small ball O_1 around m_1:*

$$\varrho_{O_2}(y) \;=\; \inf\{t > 0 \,|\, y(t) \in O_2,\, y(0) = y \in O_1\}.$$

Transition Rate Matrix

Our goal is to build a two-state Markov chain on the state space $\mathbf{S} = \{1, 2\}$, and view inter-well transitions of the diffusion as simple jumps of this chain. In [41, 20] it is shown that exit times are asymptotically almost exponential random variables. As a consequence, the asymptotic decay rate is specified as the reciprocal of the expected exit time. This enables us to obtain the jump rates for the reduced two-state Markov chain as the inverse of the asymptotic formulas (2.15)&(2.16).

As the rate matrix $\mathcal{Q} = (q_{ij})_{i,j\in\mathbf{S}}$ has to represent the infinitesimal generator for an approximating Markov chain, we have to consider the following simple rules in the construction:

(i.) for every $i \in \mathbf{S}$ we have $q_{ii} < 0$;

(ii.) $q_{ij} \geq 0$ for $i \neq j$;

(iii.) $\sum_{j\in\mathbf{S}} q_{ij} = 0$ for all $i \in \mathbf{S}$;

(iv.) $\mathcal{Q}$ generates a unique invariant density.

The second and the third condition guarantee that $\mathcal{Q}$ generates a stochastic matrix $\exp(t\mathcal{Q})$ for all $t \geq 0$, the entries of which are the respective transition probabilities to jump from one state to the other at time t. In the case considered here, the state-space is two-dimensional, $\mathbf{S} = \{1, 2\}$, and the transition rates from $1 \to 2$ and from $2 \to 1$ are easily obtained by the inverse of the asymptotically derived mean transition times $\mathcal{T}_{1\to 2}$ and $\mathcal{T}_{2\to 1}$ specified in (2.15)&(2.16). Therefore, we set $q_{12} = 1/\mathcal{T}_{1\to 2}$ and $q_{21} = 1/\mathcal{T}_{1\to 2}$, such that the rate matrix $\mathcal{Q}$ is defined by

$$\mathcal{Q} \;=\; \begin{pmatrix} -1/\mathcal{T}_{1\to 2} & 1/\mathcal{T}_{1\to 2} \\ 1/\mathcal{T}_{2\to 1} & -1/\mathcal{T}_{2\to 1} \end{pmatrix}, \qquad \mathcal{Q}\begin{pmatrix} 1 \\ 1 \end{pmatrix} = 0. \tag{2.17}$$

The (assumed positive and unique) invariant density $\psi = (\psi_1, \psi_2)^T$ is determined as the (unique) solution of

$$\mathcal{Q}^T \psi \;=\; 0 \qquad \text{with } \psi_1 + \psi_2 \,=\, 1.$$

It is natural to suppose that explicit values for the invariant density ψ are derived by the weights of the respective potential wells, for the two-state Markov chain copies the inter-well transition of the process (2.14). That is, we expect the invariant density to be given by

$$\psi_1 \,=\, \mu(B_1) \,=\, \int_{B_1} \mu(y)\,\mathrm{d}y, \qquad \psi_2 \,=\, \mu(B_2) \,=\, \int_{B_2} \mu(y)\,\mathrm{d}y.$$

To establish the above expectation, we simply have to verify

$$\frac{\mu(B_2)}{\mu(B_1)} \,=\, \frac{\mathcal{T}_{2\to 1}}{\mathcal{T}_{1\to 2}} \qquad \Big(\Rightarrow \mathcal{Q}^T \begin{pmatrix} \mu(B_1) \\ \mu(B_2) \end{pmatrix} \,=\, 0 \Big). \tag{2.18}$$

To this end, we may apply Laplace's method of asymptotic evaluation of integrals depending on the parameter ς. According to Laplace (see Appendix D), we easily get the asymptotic estimates in the small noise limit

$$\frac{\mu(B_2)}{\mu(B_1)} \;\doteq\; \sqrt{\frac{\omega_1}{\omega_2}}\, \exp\big(-\frac{2}{\varsigma^2}(V(m_2) - V(m_1))\big), \tag{2.19}$$

and, by using $V(m_2) - V(m_1) = -(V^2_{\mathrm{bar}} - V^1_{\mathrm{bar}})$ together with (2.15)&(2.16), we end up with

$$\frac{\mu(B_2)}{\mu(B_1)} \,\simeq\, \frac{\mathcal{T}_{2\to 1}}{\mathcal{T}_{1\to 2}}.$$

To express the rate matrix in terms of the invariant density, we shall investigate the second eigenvalue λ_1 of the infinitesimal generator that corresponds to the diffusion process (2.14) for small values of ς. It is well known that the dominant spectrum of the generator serves as a quantity for the exchange rates between metastable subsets of the system. Thus, the assumed double-well structure of the potential V implies the dominant spectrum to consist of two eigenvalues, $\lambda_0 = 0$ and $0 \approx \lambda_1 \in \mathbf{R}^-$, while the remainder is bounded away by a large spectral gap. The informations about the behaviour of λ_1 are again based on the results of Pavlyukevich in [36] who derived the asymptotic formula of λ_1 in the small noise limit by expanding λ_1 into a power series. The refinement for *asymmetric* double-well potential gives the accurate asymptotics for λ_1 in terms of quantities concerning the *shallow* well of the potential:

$$|\lambda_1| \;\doteq\; \frac{\sqrt{w_1\,\omega_0}}{2\pi}\, \exp\big(-\frac{2}{\varsigma^2} V^1_{\mathrm{bar}}\big).$$

This result has been derived for asymmetric double-well potentials, such that the weight on the deep well is approximately 1, that is, $\mu(B_2) \approx 1$. This obviously is fulfilled for small values of ς due to $\mu(B_2) \to 1$ as $\varsigma \to 0$. However, to include the case of symmetric double-well potentials (then we have $\mu(B_2) = \mu(B_1) = 0.5$) we prefer to rewrite the asymptotics of λ_1 according to

$$|\lambda_1|\,\mu(B_2) \;\doteq\; \frac{\sqrt{w_1\,\omega_0}}{2\pi}\,\exp(-\frac{2}{\varsigma^2}V^1_{\rm bar}),$$

which allows us due to (2.15) to express the transition rate q_{12} from $1 \to 2$ equivalently by $q_{12} = |\lambda_1|\mu(B_2)$. Using the invariant density ψ of the transition rate matrix provides us with an alternative formulation for the asymptotics of λ_1 by using the curvature in the deep well (and the weight over the shallow well):

$$|\lambda_1|\,\mu(B_1) \;\doteq\; \frac{\sqrt{w_2\,\omega_0}}{2\pi}\,\exp(-\frac{2}{\varsigma^2}V^2_{\rm bar}).$$

Summarisingly, we have

$$\mathcal{T}_{1\to 2} \simeq \frac{1}{|\lambda_1|\mu(B_2)}, \qquad \mathcal{T}_{2\to 1} \simeq \frac{1}{|\lambda_1|\mu(B_1)},$$

such that the transition rate matrix $\mathcal{Q}$ asymptotically is equivalently expressed as

$$\mathcal{Q} \;\simeq\; \begin{pmatrix} -|\lambda_1|\mu(B_2) & |\lambda_1|\mu(B_2) \\ |\lambda_1|\mu(B_1) & -|\lambda_1|\mu(B_1) \end{pmatrix}. \tag{2.20}$$

In this representation, the rate matrix exactly corresponds[5] to the exchange term (1.19) for the conditionally averaged system (1.21) that governs the jumps of the two state Markov chain $I(t,x)$. However, as will become apparent in Section 3.5.1, the rate matrix given in (1.19) has to be considered as the generator of the transition matrix propagating densities that are normalized relative to $\big(\mu(B_x^{(1)}), \mu(B_x^{(2)})\big)^T$. To help orient the reader, we close this section with some general comments on the ensemble description of finite state Markov chains.

Remark 2.2.3 *The rate matrix $\mathcal{Q}$ is basically considered to be part of the backward Kolmogorov equation $\partial_t \vec{d} = \mathcal{Q}\vec{d}$, $\vec{d} = (d_1, d_2, ..., d_N)^T \in \mathbf{R}^N$, that is, it describes the evolution of the expectations of functions of the state of the system. The evolution of (physical) probability vectors is described by the forward Fokker-Planck equation $\partial_t \vec{d} = \mathcal{Q}^T\vec{d}$ with generator*

[5] Apart form the x-dependence of the eigenvalue and the weights. Moreover, we do not know yet, if $B_x^{(1)}$ and $B_x^{(2)}$ from (1.14) are given by the saddle point of the potential.

$\mathcal{Q}^T$. *Let* $\psi = (\psi_1, ..., \psi_N)^T$ *denote a probability vector (not necessarily invariant). Let us now switch to the equivalent description in the* ψ*-weighted space* $l^2(\psi)$ *endowed with the* ψ*-weighted inner product* $\langle f, g\rangle_\psi = f^T D g$ *with* $f = (f_1, f_2, ..., f_N)^T$, $g = (g_1, ..., g_N)^T$ *and* D *defined by* $D = \mathrm{diag}(\psi)$. *The evolution of expectations of functions in* $l^2(\psi)$ *still is given by* $\partial_t \vec{d} = \mathcal{Q}\vec{d}$, *whereas the Fokker-Planck equation in the weighted space is obtained by transforming* $\mathcal{Q}$ *according to*

$$\widehat{\mathcal{Q}} \;=\; D^{-1}\mathcal{Q}^T D. \tag{2.21}$$

With it the evolution of densities normalized relative to ψ *is now described by* $\partial_t \vec{d} = \widehat{\mathcal{Q}}\vec{d}$, *and we have* $\mathcal{Q} = \widehat{\mathcal{Q}}$ *iff* $\mathcal{Q}$ *is self-adjoint wrt. the inner product* $\langle\cdot,\cdot\rangle_\psi$. *As a necessary condition for* $\mathcal{Q} = \widehat{\mathcal{Q}}$ *we obtain that* ψ *has to be the (assumed unique) invariant density of* $\mathcal{Q}$, *hence* $\mathcal{Q}^T\psi = 0$.

For $\mathbf{S} = \{1, 2\}$, *things are considerably easier to sort out. We define the rate matrix* $\mathcal{Q}$ *by*

$$\mathcal{Q} = \begin{pmatrix} -a & a \\ b & -b \end{pmatrix}, \qquad a,\, b > 0, \tag{2.22}$$

and denote $l^2(\psi)$ *with* $\psi = (\psi_1, \psi_2)^T$ *the weighted space with inner product* $\langle\cdot,\cdot\rangle_\psi$. *As before,* $\widehat{\mathcal{Q}}$ *is the generator that corresponds to the Fokker-Planck equation in* $l^2(\psi)$ *and* $D = \mathrm{diag}(\psi)$. *According to (2.21) we now obtain*

$$\widehat{\mathcal{Q}} \;=\; \begin{pmatrix} -a & b(\psi_2/\psi_1) \\ a(\psi_1/\psi_2) & -b \end{pmatrix},$$

which results in

$$\widehat{\mathcal{Q}} = \mathcal{Q} \quad\Longleftrightarrow\quad \frac{\psi_1}{\psi_2} = \frac{b}{a} \quad\Longleftrightarrow\quad \mathcal{Q}^T\psi = 0.$$

Consequently, the generator $\widehat{\mathcal{Q}}$ *will take the form of a rate matrix if and only if* ψ *is the stationary probability density of the transition process that is generated by* $\mathcal{Q}$.

In the next subsection we illustrate the validity of the asymptotic formulas (2.15)&(2.16) through results from numerical experiments that reveal that the approximation is even valid for moderate values of ς.

Numerical Illustration of Exit Times/Rates

Here, we numerically compute the quantities from the last two subsections that correspond to the diffusion process (2.14). To this end we use the asymmetric double-well potential $V = V(y)$ shown in Figure 2.3:

$$V(y) \;=\; 2.5 \cdot (y^2 - 1)^2 \;-\; 1.6\, y^3 \;+\; 2.4,$$

where the local minimum in the shallow well is $m_1 \approx -0.7884$ and the right minimum is $m_2 \approx 1.2684$. For the potential barriers we have $V_{\text{bar}}^1 \approx 1.3579$ and $V_{\text{bar}}^2 \approx 4.8383$.

Table 2.1 shows the estimated mean exit times from $B_1 + \delta$ for different values of δ by means of $N = 1000$ realizations. The initial value is chosen $y(t = 0) = -0.78 \approx m_1$. Comparing the computed values with the asymptotic estimate in formula (2.15) actually reveals that the formula rather estimates the stopping times that are defined by exiting B_1 *and* entering some region of attraction to m_2. This is equivalent to $\bar{\tau}_{B_1+\delta}$ with $\delta > 0$. These considerations will apply as well to the exits from the deep well at

	$\varsigma = 1.5$	$\varsigma = 1.0$	$\varsigma = 0.8$	$\varsigma = 0.7$	$\varsigma = 0.65$	$\varsigma = 0.6$
$\mathcal{T}_{1\to 2}$	1.65	7.46	34.37	126	305	932
$\bar{\tau}_{B_1}$	1.06	5.30	22.5	83	202	605
$\bar{\tau}_{B_1+0.2}$	1.53	7.45	32.24	129	305	907
$\bar{\tau}_{B_1+0.4}$	1.84	8.58	36.66	130	320	961
$\bar{\tau}_{B_1+0.8}$	1.90	8.55	38.30	135	310	940

Table 2.1: Mean exit times from the shallow well for different values of ς: In the first row we show the precise asymptotic estimate for the metastable exit times according to (2.15); the rows below illustrate the computed mean exit times from $B_1 + \delta$ for $\delta = 0, 0.2, 0.4, 0.8$ by means of $N = 1000$ realizations.

the right side of the saddle point. Therefore, we choose a priori $\delta = 0.4$ and compute the mean exit times from $B_2 - \delta$ for different values of ς by means of $N = 1000$ realizations with starting point $y(t = 0) = 1.2 \approx m_2$. The results displayed in Table 2.2 perfectly agree with the precise estimate via formula (2.16) even for moderately small values of ς. Table 2.2 shows that

	$\varsigma = 1.5$	$\varsigma = 1.2$	$\varsigma = 1.15$	$\varsigma = 1.0$	$\varsigma = 0.95$
$\mathcal{T}_{2\to 1}$	28.70	322	586	6201	17640
$\mathcal{T}_{1\to 2}\mu(B_2)/\mu(B_1)$	27.58	300	544	5795	16561
$\bar{\tau}_{B_2-0.4}$	26.23	305	573	5690	18490

Table 2.2: Mean exit times from the deep well for different values of ς: In the first row we show the precise asymptotic estimate for the metastable exit times according to (2.16); the second row illustrates the values obtained by formula (2.15) and the numerically computed weights; in the row below we compare these values to the numerically derived mean exit times by means of $N = 1000$ realizations.

the metastable transitions from the deep to the shallow well are equally well approximated by means of the stationary density $\psi = (\mu(B_1), \mu(B_2))^T$ of the rate matrix $\mathcal{Q}$ together with the mean transition from the shallow to the

deep well.

Finally, we incorporate into our numerical considerations the second eigenvalue λ_1 for different values of ς. It is computed by means of discretizing the corresponding generator. Table 2.3 compares the asymptotic formulas (2.15)&(2.16) for $\mathcal{T}_{1\to 2}$ and $\mathcal{T}_{2\to 1}$ with the inverse of $|\lambda_1|\mu(B_i)$, $i = 1, 2$. It nicely illustrates that λ_1 is obtained as well by using the the metastable

	$\varsigma = 1.5$	$\varsigma = 1.2$	$\varsigma = 1.0$	$\varsigma = 0.8$	$\varsigma = 0.7$	$\varsigma = 0.6$
$\lvert\lambda_1\rvert$	0.6147	2801	0.1203	0.0267	0.0074	0.0010
$1/\lvert\lambda_1\rvert$	1.63	3.57	8.31	37.43	135	978
$\mathcal{T}_{1\to 2}$	1.65	3.25	7.46	34.37	126	932
$1/(\lambda_1\mu(B_2))$	1.72	3.61	8.32	37.43	135	978
$\mathcal{T}_{2\to 1}$	28.69	322	6201	1.4335e6	1.4673e8	1.8350e11
$1/(\lvert\lambda_1\rvert\mu(B_1))$	28.81	332	6466	1.4941e6	1.5214e8	1.8869e11

Table 2.3: Comparison of transition times by means of the asymptotic estimates (2.15)&(2.16) with transition times obtained by second eigenvalue and corresponding weights: The second eigenvalue λ_1 is computed by discretizing the infinitesimal generator.

transition time $\mathcal{T}_{2\to 1}$ from the deep to the shallow well and the weight $\mu(B_1)$ over the shallow potential well:

$$\mathcal{T}_{2\to 1} \approx \frac{1}{|\lambda_1|\mu(B_1)} \quad \Longrightarrow \quad |\lambda_1| \approx \frac{1}{\mathcal{T}_{2\to 1}\mu(B_1)}.$$

To provide pictures instead of numbers, we show a typical realization of (2.14) for $\varsigma = 1.2$ in Figure 2.4 below and compare it to the reducing Markov chain model that mimics the inter-well transitions of the process. At the top we show the original process and at the bottom the numerical realization of the transition rate matrix $\mathcal{Q}$ according to (2.17). We clearly observe distributional coincidence between the inter-well transitions of $y(t)$ and the jumps generated by $\mathcal{Q}$.

Coupling Noise Intensity to Smallness Parameter ϵ

If we introduce the time scale transformation $t \mapsto t/\epsilon$, the Smoluchowski equation (2.14) is rescaled to the stochastic differential equation

$$\dot{y}^\epsilon \;=\; -\frac{1}{\epsilon} D_y V(y) \;+\; \frac{1}{\sqrt{\epsilon}}\,\varsigma\,\dot{W}, \tag{2.23}$$

and the results of the last subsections have to be modified wrt. the smallness parameter ϵ. Therefore, we have to set $\tau_D \mapsto \tau_D^\epsilon = \epsilon\,\tau_D$ for the first exit time from some subset D of the state space. The expected (metastable)

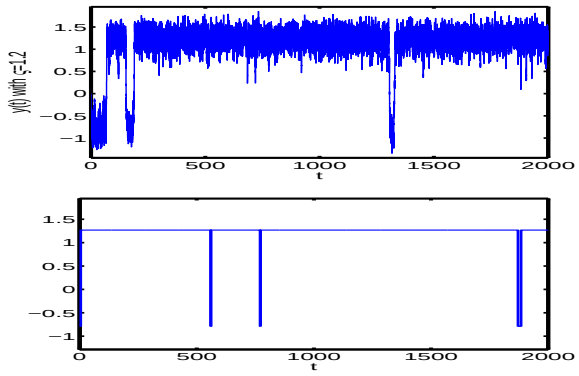

Figure 2.4: Inter-well transitions of process (2.14) compared to sample paths of Markov chain model corresponding to $\mathcal{Q}$ (bottom). $\mathcal{Q}$ seems to render satisfactorily the jumps between the potential wells.

transition times between the potential wells are now given by the precise asymptotic estimates

$$\mathcal{T}^{\epsilon}_{1\to 2} \simeq \epsilon \frac{2\pi}{\sqrt{w_1\,\omega_0}} \exp(\frac{2}{\varsigma^2} V^1_{\text{bar}}), \tag{2.24}$$

$$\mathcal{T}^{\epsilon}_{2\to 1} \simeq \epsilon \frac{2\pi}{\sqrt{w_2\,\omega_0}} \exp(\frac{2}{\varsigma^2} V^2_{\text{bar}}), \tag{2.25}$$

and the corresponding transition rate matrix $\mathcal{Q}^{\epsilon}$ takes the form

$$\mathcal{Q}^{\epsilon} = \frac{1}{\epsilon}\,\mathcal{Q} = \begin{pmatrix} -1/\mathcal{T}^{\epsilon}_{1\to 2} & 1/\mathcal{T}^{\epsilon}_{1\to 2} \\ 1/\mathcal{T}^{\epsilon}_{2\to 1} & -1/\mathcal{T}^{\epsilon}_{2\to 1} \end{pmatrix}.$$

The rate matrix $\mathcal{Q}^{\epsilon}$ generates a Markov chain that is suitable to approximate the inter-well transitions of the dynamics (2.23). The intra-well small fluctuations of the diffusion in the potential minima can be approximated by OU processes. Both approaches (inter-well and intra-well) are mathematically justified in the limit of small noise intensity ς.

Therefore, the request for vanishing approximation errors suggests to send ς to zero as $\epsilon \to 0$. This will effect another important concern of our investigations. Recalling our primary goal of justifying the need of Conditional Averaging, we recommend to freeze the fast scale effects on a time scale of order ord(1) being expressed in (2.4). According to (2.24)&(2.25), this can explicitly be realized only if $\exp(-(2/\varsigma^2)\Delta V)$ scales like ϵ. Here, ΔV denotes the barrier that has to be crossed, that is, $\Delta V = V^1_{\text{bar}}$ or $\Delta V = V^2_{\text{bar}}$. A natural way of deriving (2.4) was to rescale the potential energy barrier in an appropriate manner (this will be done in Section 3.5.3). However, the approximation of the fast dynamics by OU processes requires $\varsigma \to 0$, such that we leave the potential untouched and rescale the diffusion ς instead.

An easy calculation reveals the following situations:

$$\mathcal{T}^{\epsilon}_{1\to 2} \simeq C_1 = \mathrm{ord}(1) \iff \varsigma(\epsilon) \simeq \Big(\frac{2V^1_{\mathrm{bar}}}{\ln(K_1/\epsilon)}\Big)^{1/2}, \tag{2.26}$$

$$\mathcal{T}^{\epsilon}_{2\to 1} \simeq C_2 = \mathrm{ord}(1) \iff \varsigma(\epsilon) \simeq \Big(\frac{2V^2_{\mathrm{bar}}}{\ln(K_2/\epsilon)}\Big)^{1/2}, \tag{2.27}$$

for some $K_i > 0$, $i = 1, 2$. Note, that we really have to define ς by using the asymptotic equality and not the (asymptotic) order ord[6]. To overcome the problem of different potential barrier heights $V^1_{\mathrm{bar}} < V^2_{\mathrm{bar}}$, we basically have two possibilities each of which means to accept a somehow unaestethic modification: Firstly, we accept that ς will additionally depend on the attractor basins of the process, that is $\varsigma = \varsigma(\epsilon, i)$ with $i \in \mathbf{S} = \{1, 2\}$. This allows us to obtain $\mathcal{T}^{\epsilon}_{1\to 2} = \mathrm{ord}(1)$ as well as $\mathcal{T}^{\epsilon}_{2\to 1} = \mathrm{ord}(1)$. If we want to avoid the additional dependence of ς on the potential wells $i = \{1, 2\}$, we have to elect (2.26) *or* (2.27), such that we cannot comply with both requirements. According to $(1 + \delta)V^1_{\mathrm{bar}} = V^2_{\mathrm{bar}}$ for some $\delta > 0$, we then get $\mathcal{T}^{\epsilon}_{1\to 2} = \mathrm{ord}(1) \Rightarrow \mathcal{T}^{\epsilon}_{2\to 1} = \mathrm{ord}(\epsilon^{-\delta})$. Vice versa, for $\mathcal{T}^{\epsilon}_{2\to 1} = \mathrm{ord}(1)$ we obtain $\mathcal{T}^{\epsilon}_{1\to 2} = \mathrm{ord}(\epsilon^{\delta})$. However, as we want to freeze both transition times, it is natural to use (2.26) instead of (2.27). Only in this case we obtain $\lambda^{\epsilon}_1 = \mathrm{ord}(1)$ for the most dominant eigenvalue $\lambda^{\epsilon}_1 < 0$ of the corresponding generator, because we asymptotically have

$$\lambda^{\epsilon}_1 \simeq -\frac{1}{\mu(B_2)\mathcal{T}^{\epsilon}_{1\to 2}}.$$

Consequently, we suggest to freeze the transitions from the shallow to the deep well on a time scale $t \sim 1$ to guarantee that the second eigenvalue λ^{ϵ}_1 asymptotically is part of the dominant spectrum.

2.2.3 Full Dynamics Approach

Let us now return to the full dynamics description according to (2.1)&(2.2). The previous results allow us to reduce the essential dynamics of the fast diffusion (2.2) in a double-well potential to a two-state Markov chain that carries information about the inter-well transitions, whereas the intra-well small fluctuations in the potential minima are approximated by an OU process, respectively. The approach is justified for vanishing noise intensity

[6] For example, if we had

$$\varsigma(\epsilon) = k\Big(\frac{2V^1_{\mathrm{bar}}}{\ln(K/\epsilon)}\Big)^{1/2} \implies \varsigma(\epsilon) = \mathrm{ord}\Big(\Big(\frac{2V^1_{\mathrm{bar}}}{\ln(K/\epsilon)}\Big)^{1/2}\Big).$$

However, for $0 < k \neq 1$ this implies

$$\mathcal{T}^{\epsilon}_{1\to 2} = \mathrm{ord}(\epsilon/\epsilon^k) \neq \mathrm{ord}(1).$$

$\varsigma = \varsigma(\epsilon) \to 0$ as $\epsilon \to 0$. The final step is to incorporate the slow variable dynamics (2.1) into the procedure. To this end, the only task is to adapt the notation to the full dynamics situation where the fast process necessarily depends on x such that the quantities (as exit times/rates, metastable sets) from the last sections have to be indexed with the fixed variable x, respectively.

Recapitulating: The system under consideration is the Smoluchowski equation in a slow variable, x, and a fast one, y:

$$\dot{x}^\epsilon = -D_x V(x,y) + \sigma \dot{W}_1 \tag{2.28}$$

$$\dot{y}^\epsilon = -\frac{1}{\epsilon} D_y V(x,y) + \frac{\varsigma(\epsilon)}{\sqrt{\epsilon}} \dot{W}_2, \tag{2.29}$$

for a given potential $V : \mathbf{R}^{m+1} \to \mathbf{R}^+$ satisfying Assumption 2.2.1 and $\varsigma(\epsilon) \to 0$ as $\epsilon \to 0$. Thus, the full dynamics state space can be basically decomposed into two metastable subsets $B^{(1)} \cup B^{(2)}$, where the metastability originates from the fast diffusion process due to the double-well structure of $V(x,\cdot)$. In this direction $B_x^{(i)}$ denotes the restriction of $B^{(i)}$ to the fibre $\Phi(x) = \{(x,y) \mid y \in \mathbf{R}\}$, such that $B_x^{(1)} = \{(x,y) \mid y < 0\}$ and $B^{(2)} = \{(x,y) \mid y > 0\}$ where the boundary is given by the saddle point $y_0 = 0$. Then, the full dynamics process (x^ϵ, y^ϵ) can be decomposed into two almost irreducible subprocesses, such that the rare changes from one subprocess to the other are induced by the y dynamics. In this case (when the transitions do not happen along the x direction), we can reduce the transition process to a continuous-time two-state Markov chain $I(t,x) \in \mathbf{S} = \{1,2\}$ that is generated by the rate matrix $\mathcal{Q}_x = (q_{ij}^\epsilon(x))_{ij \in \mathbf{S}}$ depending on the position of the slow variable[7]. The entries of $\mathcal{Q}_x$ are specified explicitly by the inverse of the asymptotic inter-well mean transition times:

$$\begin{aligned}
q_{11}^\epsilon(x) &= -q_{12}^\epsilon(x), \qquad q_{22}^\epsilon(x) = -q_{21}^\epsilon(x), \\
q_{12}^\epsilon(x) &= \frac{1}{\mathcal{T}_{1\to 2}^\epsilon(x)} = \frac{1}{\epsilon}\frac{1}{\mathcal{T}_{1\to 2}(x)} \simeq \frac{1}{\epsilon}\frac{\sqrt{\omega^{(1)}(x)\omega_0(x)}}{2\pi}\exp(-\frac{2}{\varsigma^2}V_{\mathrm{bar}}^{(1)}(x)), \\
q_{21}^\epsilon(x) &= \frac{1}{\mathcal{T}_{2\to 1}^\epsilon(x)} = \frac{1}{\epsilon}\frac{1}{\mathcal{T}_{2\to 1}(x)} \simeq \frac{1}{\epsilon}\frac{\sqrt{\omega^{(2)}(x)\omega_0(x)}}{2\pi}\exp(-\frac{2}{\varsigma^2}V_{\mathrm{bar}}^{(2)}(x)).
\end{aligned} \tag{2.30}$$

Note that the transition rate from $2 \to 1$ is asymptotically equally well expressed as

$$q_{21}^\epsilon(x) \simeq q_{12}^\epsilon(x)\frac{\mu_x(B_x^{(1)})}{\mu_x(B_x^{(2)})},$$

[7] We desist from indexing $\mathcal{Q}_x$ with ϵ, for the averaging procedure in the next section is performed without considering the ϵ-dependence of $\mathcal{Q} = \mathcal{Q}_x$.

with $\mu_x^{(i)}$ given in (2.11). For decreasing smallness parameter ϵ, the dynamics (2.28)&(2.29) are well approximated by

$$\dot{x}^\epsilon = -D_x V(x, y_{\mathrm{OU}}) + \sigma \dot{W}_1 \tag{2.31}$$

$$\dot{y}^\epsilon_{\mathrm{OU}} = -\frac{1}{\epsilon}\,\omega^{(I(t,x))}(x)\big(y_{\mathrm{OU}} - m^{(I(t,x))}(x)\big) + \frac{\varsigma(\epsilon)}{\sqrt{\epsilon}}\dot{W}_2, \tag{2.32}$$

with $I(t,x) \in \mathbf{S} = \{1,2\}$ denoting the x-dependent Markov chain model which is described by the transition rate matrix $\mathcal{Q}_x$.

Coupling Noise Intensity to Potential Energy Barrier

In the last paragraph of Section 2.2.2 we pointed out how to couple the diffusion term $\varsigma(\epsilon)$ to ϵ such that metastability in the fast dynamics is preserved for decreasing ϵ and fixed slow variable x. As an indicator for metastability we use the second eigenvalue $\lambda_1^\epsilon = \lambda_1^\epsilon(x)$ of the corresponding generator for fixed x. Equivalently we can consider the x-dependent transition times from the shallow to the deep well of the potential $V(x,\cdot)$. Thus, to freeze these transition times for every x it is convenient to set

$$\varsigma = \varsigma(\epsilon, x) = \left(\frac{2\min\{V_{\mathrm{bar}}^{(i)}(x) \mid i = 1,2\}}{\ln(K/\epsilon)}\right)^{1/2}, \qquad K > 0, \tag{2.33}$$

with $V_{\mathrm{bar}}^{(1)}(x)$ denoting the potential barrier in the left well, $V_{\mathrm{bar}}^{(2)}(x)$ denoting the barrier in the right well.

Remark 2.2.4 *The principal physical feature of functioning of biomolecules is that they operate at ambient temperature and solvent condition, and most biomolecular processes can only be understood in a thermodynamical context. Therefore, most experiments on biomolecular systems are performed under the equilibrium conditions of constant temperature T, particle number, and volume. For the Smoluchowski system (2.28)&(2.29) this means to enforce $\sigma = \varsigma$ (for fixed ϵ), such that experiments can be arranged with inverse temperature $\beta = -2/\varsigma^2$. However, if the noise intensity ς depends on the slow variable x by means of (2.33), it is hardly possible to interpret the model system in the context of equilibrium ensembles. Therefore, the suggestion (2.33) is not satisfactory as its application removes the system under consideration from the context of mathematical modeling of biological processes. We will show in Section 2.2.5 how to avoid coupling of the diffusion ς to x and still obtain large time conformational changes in the asymptotic limit $\epsilon \to 0$.*

2.2.4 From Dynamics With OU Processes to OU-Averaged Dynamics

By coupling the diffusion term ς in the fast dynamics (2.29) to the parameter ϵ under (2.33), we obtain that the original dynamics exhibit *three* timescales:

the fast scale of motion in y, the slow scale of motion in x, and the scale of rare transitions between the metastable sets in y. In this case the standard averaging scheme will fail if we apply it to the original dynamics given by (2.28)&(2.29). Insensitivity of the averaging procedure with respect to the slow mixing between the metastable fast dynamics then can lead to an underestimation of the metastable transitions of the slow dynamics. However, application of the averaging method to the system with OU processes will not mix up the fast scale effects that are represented by the reducing two-state Markov chain on the skeleton space $\mathbf{S} = \{1, 2\}$ for the inter-well transitions. We will now show that multiscale asymptotics wrt. the smallness parameter ϵ leads to an averaged model which describes the effective motion of the slow DOF statistically correct. As the method is applied to ensemble instead of single dynamics we have to set up before the necessary requirements concerning the evolution of probability densities.

Let us extend the fast-slow system with two OU processes to a finite number of OU processes. Thus, we consider for $x \in \mathbf{R}^m, y \in \mathbf{R}$ the following SDE:

$$\dot{x}^\epsilon(t) \;=\; -D_x V(x, y_{\mathrm{OU}}) \,+\, \sigma \dot{W}_1, \tag{2.34}$$

$$\dot{y}^\epsilon_{\mathrm{OU}}(t) \;=\; -\frac{1}{\epsilon}\,\omega^{(I(t,x))}(x) \cdot \big(y_{\mathrm{OU}} - m^{(I(t,x))}(x)\big) \,+\, \frac{\varsigma(x)}{\sqrt{\epsilon}} \dot{W}_2, \tag{2.35}$$

where $I(t, x)$ is a right-continuous Markov chain on a probability space taking values in a finite state space $\mathbf{S} = \{1, 2, ..., N\}$ and $\omega^{(i)}(x)$ takes values in $\mathbf{R}^+$ for all $i \in \mathbf{S}$. The noise intensity of the fast diffusion may depend on x, but is assumed to be strictly positive, that is $\varsigma(x) \geq c > 0$. To simplify notation we perform the asymptotic procedure without a possible dependence of ς on the Markov chain $I(t, x)$; a generalization in this direction had no effect on the computation. The generator $\mathcal{Q}_x = (q_{ij}(x))_{N\times N}$ of the switching chain $I(t, x)$ depends on the slow variable x and contains the transition rates $q_{ij} = q_{ij}(x) > 0$ from i to j if $i \neq j$ while

$$q_{ii}(x) \;=\; -\sum_{i\neq j} q_{ij}(x). \tag{2.36}$$

For fixed $x \in \mathbf{R}^m$ and $i \in \mathbf{S}$ the diffusion dynamics (2.35) is known as OU process and consequently ergodic. The (unique) stationary density $\mu_x^{\mathrm{OU}(i)}$ is given by

$$\mu_x^{\mathrm{OU}(i)}(y) \;=\; \frac{1}{\varsigma(x)} \sqrt{\frac{\omega^{(i)}(x)}{\pi}}\, \exp\Big(-\omega^{(i)}(x) \frac{\big(y - m^{(i)}(x)\big)^2}{\varsigma(x)^2} \Big), \tag{2.37}$$

which is a Gaussian with mean $m^{(i)}(x)$ and variance $\varsigma(x)^2/(2\omega^{(i)}(x))$, and thus independent of ϵ.

The evolution of probability densities $p^\epsilon \in L^1(\mathbf{R}^{m+1} \times \mathbf{S})$ under the dynamics given by (2.34)&(2.35) is described by the forward *Fokker-Planck*

equation. Note that in contrast to (1.3) we are now working in unweighted function spaces[8], that is, the density p^ϵ gives the physical probability to find the system in state (x, y) at time t, whereas ρ^ϵ in (1.3) denotes the density normalized relative to the invariant density μ. However, the full dynamics (2.34)&(2.35) in general will not admit an invariant density, such that we have to perform the procedure by means of the probability densities in $L^1(\mathbf{R}^{m+1}\times\mathbf{S})$. For systems that admit a unique invariant density μ, a nice description of the equivalent pictures is given in [19, Sections 1 and 2]. For later use it may be helpful to slightly change notation for the densities p^ϵ: The agreement $p^\epsilon_{(i)}(t,x,y) := p^\epsilon(t,x,y,i)$ enables us to represent p^ϵ as an N-dimensional vector according to $p^\epsilon = (p^\epsilon_{(1)},...,p^\epsilon_{(N)})$ with $p^\epsilon_{(i)} \in L^1(\mathbf{R}^{m+1})$. Now, the Fokker-Planck equation is regarded on some suitable subspace of $L^1(\mathbf{R}^{m+1}\times\mathbf{S})$, and reads[9]

$$\begin{aligned} \partial_t p^\epsilon &= \mathcal{A}^\epsilon p^\epsilon \\ \mathcal{A}^\epsilon &= \frac{1}{\epsilon}\mathcal{A}_x + \mathcal{A}_y + \mathcal{Q}^T \end{aligned} \tag{2.38}$$

$$\mathcal{A}_x = \begin{pmatrix} \mathcal{A}_x^{(1)} & 0 & 0 & 0 \\ 0 & \mathcal{A}_x^{(2)} & 0 & 0 \\ 0 & 0 & \ddots & 0 \\ 0 & 0 & 0 & \mathcal{A}_x^{(N)} \end{pmatrix}, \mathcal{A}_y = \begin{pmatrix} \mathcal{A}_y^{(1)} & 0 & 0 & 0 \\ 0 & \mathcal{A}_y^{(2)} & 0 & 0 \\ 0 & 0 & \ddots & 0 \\ 0 & 0 & 0 & \mathcal{A}_y^{(N)} \end{pmatrix}$$

where $\mathcal{A}_x^{(i)}$ and $\mathcal{A}_y^{(i)}$ are given for $f \in L^1(\mathbf{R}^{m+1})$ by

$$\begin{aligned} \mathcal{A}_x^{(i)} f(x,y) &= \frac{\varsigma(x)^2}{2}\Delta_y f(x,y) + D_y\Big(\omega^{(i)}(x)\big(y - m^{(i)}(x)\big)\cdot f(x,y)\Big) \\ \mathcal{A}_y^{(i)} f(x,y) &= \frac{\sigma^2}{2}\Delta_x f + D_x\big(D_x V(x,y)\cdot f(x,y)\big). \end{aligned}$$

According to Remark 2.2.3, we actually have to use $\mathcal{Q}^T$ in (2.38), for $\mathcal{Q}$ is considered as the infinitesimal generator corresponding to the backward Chapman-Kolmogorov equation. Consequently, the probability to be in state (x, y) is given by

$$\langle p^\epsilon(t,x,y), \mathbf{1}\rangle_{\mathbf{S}} = \sum_{i\in\mathbf{S}} p^\epsilon_{(i)}(t,x,y),$$

$\langle\cdot,\cdot\rangle_{\mathbf{S}}$ denoting the Euclidean inner product in $\mathbf{R}^N$.

Our aim is to average with respect to the fast variable y and obtain an averaged equation for the slow variable x alone. To this end, we will use

[8] Therefore, we prefer to change the notation for the functions as well as for the generators.

[9] We could also perform the procedure in $L^2(\mathbf{R}^{m+1}\times\mathbf{S})$. For the Fokker-Planck equation (1.3) we prefer the weighted Hilbert space $L^2(\mu) \subset L^1(\mu)$ instead of $L^1(\mu)$, as this renders the generator self-adjoint.

multiscale analysis and give an idea of the proof in Appendix B which is based on a theorem of Kurtz.

Projection Operator

We would like to derive an equation for the distribution function in x:

$$\int \langle p^\epsilon(t,x,y), \mathbf{1}\rangle_{\mathbf{S}} \, \mathrm{d}y \;=\; \sum_{i\in\mathbf{S}} \int p^\epsilon_{(i)}(t,x,y)\, \mathrm{d}y,$$

which would be valid in the limit where ϵ becomes very small. To this end, we introduce the vector $\overline{p}^\epsilon(t,x) = (\overline{p}^\epsilon_{(1)}, ..., \overline{p}^\epsilon_{(N)})^T$ with densities $\overline{p}^\epsilon_{(i)} \in L^1(\mathbf{R}^m)$ defined by

$$\overline{p}^\epsilon_{(i)}(t,x) \;=\; \int p^\epsilon_{(i)}(t,x,y)\, \mathrm{d}y.$$

It is expected that an approximate solution of the full dynamics would be obtained by multiplying each $\overline{p}^\epsilon_{(i)}(t,x)$ by the stationary distribution $\mu_x^{\mathrm{OU}(i)}$ of the SDE (2.35) for fixed $I(t,x) = i$. We formalize this by defining a *projection operator* $\Pi = \mathrm{diag}(\Pi^{(1)}, ..., \Pi^{(N)})$ acting on functions $f = (f_1, ..., f_N)^T \in L^1(\mathbf{R}^{m+1} \times \mathbf{S})$ by

$$(\Pi f)(x,y) \;=\; \mathrm{diag}(\mu_x^{\mathrm{OU}(1)}, ..., \mu_x^{\mathrm{OU}(N)}) \int f(x,y)\, \mathrm{d}y.$$

It is obvious that Π projects any function into the subspace of all functions which can be written in the form

$$f \;=\; (f_1, ..., f_N)^T, \quad f_i(x,y) \;=\; \overline{f}_i(x) \cdot \mu_x^{\mathrm{OU}(i)}(y), \tag{2.39}$$

where $\overline{f}_i$ is an arbitrary function of $L^1(\mathbf{R}^m)$, thus $\overline{f} = (\overline{f}_1, ..., \overline{f}_N)^T \in L^1(\mathbf{R}^m \times \mathbf{S})$. In the following we study the case where the initial condition $p^\epsilon(t = 0, x, y)$ can be expressed by

$$p^\epsilon(t=0,x,y) \;=\; (\Pi p^\epsilon(t=0))(x,y).$$

However, functions f of the form (2.39) are all solutions of

$$\mathcal{A}_x f \;=\; 0,$$

that is, the space into which Π projects is the kernel or nullspace of $\mathcal{A}_x$ expressed by $\mathcal{A}_x \Pi = 0$. Due to the properties of $\mathcal{A}_x^{(i)}$ considered as an operator acting on functions g in y, that is $g = g(y) \in L^1(\mathbf{R})$, we furthermore have:

$$\Pi \mathcal{A}_x \;=\; 0 \;=\; \mathcal{A}_x \Pi. \tag{2.40}$$

This is easily seen by introducing the formal adjoint $\mathcal{T}_x^{(i)}$ of $\mathcal{A}_x^{(i)}$, i.e., a differential operator such that for all $u \in L^1(\mathbf{R})$, $v \in L^\infty$ (or $u, v \in L^2(\mathbf{R})$) we have

$$\langle \mathcal{A}_x^{(i)} u, v \rangle_{L^2} \;=\; \langle u, \mathcal{T}_x^{(i)} v \rangle_{L^2}, \qquad \langle u, v \rangle_{L^2} := \int u(y) \cdot \overline{v(y)}\, \mathrm{d}y.$$

If we consider $\Pi^{(i)}$ –for fixed x– as an operator acting on functions in y, we can rewrite it by

$$\Pi^{(i)} u \;=\; \langle u, \mathbf{1} \rangle_{L^2} \cdot \mu_x^{\mathrm{OU}(i)}.$$

Together with the well-known fact that $\mathcal{T}_x^{(i)} \mathbf{1} = 0$ (see, e.g., [19, 42]) we finally get the desired result (2.40).

Multiscale Analysis

We now make the following ansatz for the solution of the Fokker-Planck equation with the initial conditions described above:

$$p^\epsilon \;=\; p^0 \;+\; \epsilon\, p^1 \;+\; \epsilon^2\, p^2 \;+ \ldots$$

This ansatz is inserted into the Fokker-Planck equation (2.38) and then, by comparison of coefficients of different powers of ϵ we get:

$$\epsilon^{-1} \;:\quad \mathcal{A}_x\, p^0 \;=\; 0 \tag{2.41}$$

$$\epsilon^{0} \;:\quad \mathcal{A}_x\, p^1 \;+\; (\mathcal{A}_y + \mathcal{Q}^T)\, p^0 \;=\; \partial_t p^0 \tag{2.42}$$

$$\epsilon^{1} \;:\quad \mathcal{A}_x\, p^2 \;+\; (\mathcal{A}_y + \mathcal{Q}^T)\, p^1 \;=\; \partial_t p^1 \tag{2.43}$$

1. step: (2.41) immediately yields that $p^0 \in \mathcal{N}(\mathcal{A}_x)$, i.e.,

$$\begin{aligned} \Pi p^0 \;&=\; p^0, \quad \text{equivalently} \\ p^0(t,x,y) \;&=\; \mathrm{diag}(\mu_x^{\mathrm{OU}(1)}, \ldots, \mu_x^{\mathrm{OU}(N)}) \cdot \overline{p}^0(t,x), \end{aligned} \tag{2.44}$$

for a function $\overline{p}^0 \in L^1(\mathbf{R}^m \times \mathbf{S})$ depending only on x.

2. step: Let Π act on (2.42) and use (2.40). This time we get:

$$\Pi(\mathcal{A}_y + \mathcal{Q}^T)\Pi p^0 \;=\; \partial_t \Pi p^0. \tag{2.45}$$

By using (2.44) simple calculations reveal for $\overline{p}^0 = (\overline{p}^0_{(1)}, \ldots, \overline{p}^0_{(N)})^T$:

$$\partial_t \overline{p}^0 \;=\; (\overline{\mathcal{A}} \;+\; \mathcal{Q}^T)\, \overline{p}^0, \tag{2.46}$$

with

$$\overline{\mathcal{A}} = \begin{pmatrix} \overline{\mathcal{A}}^{(1)} & 0 & 0 & 0 \\ 0 & \overline{\mathcal{A}}^{(2)} & 0 & 0 \\ 0 & 0 & \ddots & 0 \\ 0 & 0 & 0 & \overline{\mathcal{A}}^{(N)} \end{pmatrix},$$

$$\overline{\mathcal{A}}^{(i)} \;=\; \frac{\sigma^2}{2}\Delta_x \;+\; D_x\Big(\int D_x V(x,y)\,\mu_x^{\mathrm{OU}(i)}(y)\,\mathrm{d}y\;\cdot\;\Big),$$

$\overline{\mathcal{A}}$ acting on $L^1(\mathbf{R}^m\times\mathbf{S})$. Thus $\overline{p}^0$ is determined by a Fokker-Planck equation, and its solution gives us p^ϵ up to error $\mathcal{O}(\epsilon)$. The associated SDE is given by

$$\dot{x}^0 \;\;=\;\; -\int D_x V(x,y)\cdot\mu_x^{\mathrm{OU}(I(t,x))}(y)\,\mathrm{d}y \;+\; \sigma\dot{W}_1, \tag{2.47}$$

where $I(t,x)\in\mathbf{S}$ controls the switches between the different OU processes due to the rate matrix $\mathcal{Q}=\mathcal{Q}_x$. The SDE (2.47) describes the limit dynamics of (2.34)&(2.35) in the sense that its solution satisfies $x^\epsilon\to x^0$ as $\epsilon\to 0$ either pathwise [15], or in the distributional sense [25, 29]. We give a formal proof of the distributional convergence in Appendix B by verifying the conditions in [25].

2.2.5 Transition Times Considered in Full State Space

In this section we come back to the problem addressed in Remark 2.2.4. To justify the approximation of the fast dynamics within each of the basins of the double-well potential by OU processes, the noise intensity ς has to be chosen very small. Therefore, we propose to relate ς to ϵ such that $\varsigma(\epsilon)\to 0$ as $\epsilon\to 0$. Simultaneously we want to attain the fast scale effects to happen on time scale ord(1) or even larger resulting in the instruction (2.33).

A simple consideration may allow us to avoid coupling ς to the slow variable dynamics x: Depending on the noise intensity σ in the slow variable dynamics (2.28), the x trajectory will stay with overwhelming probability in a bounded domain $D(\sigma)$ of its state space[10]; if we choose $V_{\mathrm{bar}}^{\mathrm{small}}$ according to the rule

$$V_{\mathrm{bar}}^{\mathrm{small}} \;\;=\;\; \min\{V_{\mathrm{bar}}^{(i)}(x)\;|\,x\in D(\sigma),\;i=1,2\},$$

and set

$$\varsigma(\epsilon) \;=\; \left(\frac{2V_{\mathrm{bar}}^{\mathrm{small}}}{\ln(K/\epsilon)}\right)^{1/2}, \qquad K\;>\;0, \tag{2.48}$$

we expect the metastable transitions to happen on a time scale $t\gtrsim 1$. If the potential energy barriers outside the domain $D(\sigma)$ are smaller than $V_{\mathrm{bar}}^{\mathrm{small}}$, the particle will for very small ϵ instantly jump over the barrier once it has reached the complement of $D(\sigma)$. Thus, the time of the metastable

[10] Note that σ is not related to ς, and we do not demand for small values of σ. However, it should be clear that a choice of $V_{\mathrm{bar}}^{\mathrm{small}}$ should depend on the actual size of σ. This becomes more clear by considering the right picture of Figure 2.5. Therefore, we write $D=D(\sigma)$ for the bounded region.

transitions will be somehow connected to the expected exit time of the x dynamics from $D(\sigma)$.

The above idea can be mathematically justified by computing the expected transition times between the metastable decomposition $B^{(1)} \cup B^{(2)}$ in the entire (x, y) state space, instead of considering the transition times on every fibre of the fast state space for fixed x. Subsequently, we restrict without loss of generality to the (metastable) expected transition time from $B^{(1)}$ to $B^{(2)}$ denoted $\overline{\mathcal{T}}^{\epsilon}_{1\to 2}$. If we choose ς according to the rule (2.48), the computation of $\overline{\mathcal{T}}^{\epsilon}_{1\to 2}$ will depend on the course of $V^{(1)}_{\mathrm{bar}}(x)$ as a function of x. To illustrate the problem, we show in Figure 2.5 two possible situations which are exemplary for the different approaches.

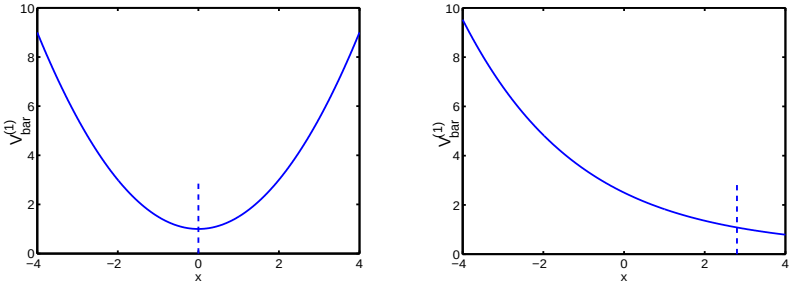

Figure 2.5: Example for the function $V^{(1)}_{\mathrm{bar}}(x)$. The dashed line indicates a point b that can be used to realize (2.48) by defining $V^{\mathrm{small}}_{\mathrm{bar}} = V^{(1)}_{\mathrm{bar}}(b)$.

For $V^{(1)}_{\mathrm{bar}}$ as illustrated at the left-hand side, we choose $V^{\mathrm{small}}_{\mathrm{bar}} = V^{(1)}_{\mathrm{bar}}(x_0)$ with $x_0 = 0$ and, according to (2.30), observe the following in the asymptotic limit $\epsilon \to 0$:

$$\begin{aligned} \mathcal{T}^{\epsilon}_{1\to 2}(x) &= \mathrm{ord}(\epsilon^{-\delta_x}), \quad x \neq x_0,\ V^{(1)}_{\mathrm{bar}}(x) = (1+\delta_x)V^{(1)}_{\mathrm{bar}}(x_0),\ \delta_x > 0, \\ \mathcal{T}^{\epsilon}_{1\to 2}(x) &= \mathrm{ord}(1), \qquad x = x_0. \end{aligned}$$

In this situation, the metastable transition time $\overline{\mathcal{T}}^{\epsilon}_{1\to 2}$ can asymptotically be derived by averaging the x-dependent transition rates[11] against the invariant probability distribution of the x dynamics restricted to the set $B^{(1)}$. The metastable transition times are then derived by taking the inverse of the averaged transition rates, that is, in the asymptotic limit $\epsilon \to 0$ we obtain $\overline{\mathcal{T}}^{\epsilon}_{1\to 2}$ according to

$$\overline{\mathcal{T}}^{\epsilon}_{1\to 2} \simeq \frac{1}{\mathbf{E}_{\bar{\mu}^{(1)}}[1/\mathcal{T}^{\epsilon}_{1\to 2}(x)]},$$

[11] Note, that we actually have to average the transition rates and *not* the transition times.

where the quantity $\mathbf{E}_{\bar{\mu}^{(1)}}[1/\mathcal{T}^{\epsilon}_{1\to 2}(x)]$ is given by

$$\mathbf{E}_{\bar{\mu}^{(1)}}[1/\mathcal{T}^{\epsilon}_{1\to 2}(x)] \;=\; \int 1/\mathcal{T}^{\epsilon}_{1\to 2}(x)\,\bar{\mu}^{(1)}(x)\,\mathrm{d}x, \tag{2.49}$$

$$\bar{\mu}^{(1)}(x) \;=\; \frac{1}{Z^{(1)}}\exp\Big(-\frac{2}{\sigma^2}\Big(-\frac{\varsigma^2}{2}\ln\int_{B_x^{(1)}}\exp(-\frac{2}{\varsigma^2}V(x,y))\mathrm{d}y\Big)\Big). \tag{2.50}$$

Here, $Z^{(1)}$ denotes the normalization constant and depends on ς as well. The derivation will become apparent later (in Chapter 3), when we justify the approach by means of multiscale analysis for distinguished time scales. Then the metastable transitions are assumed to happen on the longest time scale, which requires the averaging of the metastable transition rates (represented by the second eigenvalue of the corresponding generator) for fixed x wrt. the invariant density of the conditionally averaged potentials (cf. Section 3.3.3).

The situation shown at the right-hand side of Fig. 2.5 is somewhat different. Here, $V^{(1)}_{\mathrm{bar}}(x) \to 0$ as $x \to \infty$, and there is no local minimum $V^{\mathrm{small}}_{\mathrm{bar}}$ such that $V^{\mathrm{small}}_{\mathrm{bar}} \le V^{(1)}_{\mathrm{bar}}(x)$ for all x. Therefore, let us set $V^{\mathrm{small}}_{\mathrm{bar}} = V^{(1)}_{\mathrm{bar}}(b)$ as indicated by the dashed line in the picture and use (2.48). Then we asymptotically have

$$\begin{aligned}
\mathcal{T}^{\epsilon}_{1\to 2}(x) &= \mathrm{ord}(\epsilon^{-\delta_x}), \quad x < b,\ V^{(1)}_{\mathrm{bar}}(x) = (1+\delta_x)V^{(1)}_{\mathrm{bar}}(b),\ \delta_x > 0,\\
\mathcal{T}^{\epsilon}_{1\to 2}(x) &= \mathrm{ord}(1), \quad x = x_0,\\
\mathcal{T}^{\epsilon}_{1\to 2}(x) &= \mathrm{ord}(\epsilon^{+\delta_x}), \quad x > b,\ V^{(1)}_{\mathrm{bar}}(x) = (1-\delta_x)V^{(1)}_{\mathrm{bar}}(b),\ \delta_x > 0,
\end{aligned}$$

which implies $\mathcal{T}^{\epsilon}_{1\to 2}(x) \to 0$ for $x > b$. Here, the averaged transition rate according to (2.49) cannot be used to obtain $\overline{\mathcal{T}}^{\epsilon}_{1\to 2}$. Its application would lead to a capital underestimation of the effective transition times.

Averaged Exit Rates in the Limit of Vanishing Noise ς

To tackle the problem of evaluating the averaged transition rates, we show how to treat (2.49) by using Laplace's estimation in the limit of small noise ς. First of all, we consider the averaged density $\bar{\mu}^{(1)}(x)$: Using standard Laplacian asymptotics, we get for ς small

$$\int_{B_x^{(1)}}\exp\big(-\frac{2}{\varsigma^2}V(x,y)\big)\mathrm{d}y \;\doteq\; \varsigma\sqrt{\frac{\pi}{\omega^{(1)}(x)}}\,\exp\big(-\frac{2}{\varsigma^2}V(x,m^{(i)}(x))\big),$$

and, exploiting $(\varsigma^2/2)\ln(\varsigma\sqrt{\pi/\omega^{(1)}(x)}) \to 0$ as $\varsigma \to 0$, we end up with the asymptotic limit (from (2.50))

$$\bar{\mu}^{(1)}(x) \;\doteq\; \frac{1}{Z^{(1)}}\,\exp\big(-\frac{2}{\sigma^2}V(x,m^{(1)}(x))\big).$$

Therefore, the evaluation of (2.49) asymptotically reduces to

$$\mathbf{E}_{\bar{\mu}^{(1)}}[1/\mathcal{T}^{\epsilon}_{1\to 2}(x)] \simeq \tag{2.51}$$
$$\frac{1}{\epsilon}\,\frac{1}{Z^{(1)}}\int \frac{\sqrt{\omega^{(1)}(x)\omega_0(x)}}{2\,\pi}\exp(-\frac{2}{\varsigma^2}V^{(1)}_{\mathrm{bar}}(x))\exp(-\frac{2}{\sigma^2}V(x,m^{(1)}(x)))\,\mathrm{d}x.$$

With it we obtain for $\epsilon=\epsilon^*$ fixed $1/\,\mathbf{E}_{\bar{\mu}^{(1)}}[1/\mathcal{T}^{\epsilon^*}_{1\to 2}]\to\infty$ in the asymptotic limit $\varsigma\to 0$, which in turn implies $\mathcal{T}^{\epsilon^*}_{1\to 2}(x)\to\infty$ for almost every x. This renders the metastable transitions to happen on a time scale $t\gg 1$, which allows us to use the averaged transition rates instead for ς small.

Approach in the Limit $\epsilon\to 0$

In contrast, the situation of vanishing ϵ requires to carefully inspect the rate at which ς goes to zero together with the evolution of the barrier $V^{(1)}_{\mathrm{bar}}$ as a function of x. In so doing, we basically distinguish between the two situations reflected in Fig. 2.5:

(i.) $V^{(1)}_{\mathrm{bar}}(x)$ attains its global minimum (within the accessible state space of x) in a region where $\bar{\mu}^{(1)}$ is significantly larger than zero, that is, $V^{(1)}_{\mathrm{bar}}(x_0)=\min\{V^{(1)}_{\mathrm{bar}}(x):\,x\in\mathbf{R}\}$ and $\bar{\mu}^{(1)}(x_0)\gg 0$. If we set $V^{\mathrm{small}}_{\mathrm{bar}}=V^{(1)}_{\mathrm{bar}}(x_0)$ and couple ς to ϵ according to (2.48), we obtain

$$\overline{\mathcal{T}}^{\epsilon}_{1\to 2} \;\simeq\; 1/\,\mathbf{E}_{\bar{\mu}^{(1)}}[1/\mathcal{T}^{\epsilon}_{1\to 2}(x)] \;=\; \mathrm{ord}(\sqrt{\ln(1/\epsilon)}).$$

(ii.) The complex situation includes the case where $V^{(1)}_{\mathrm{bar}}(x)$ is strictly monotonically decreasing with $V^{(1)}_{\mathrm{bar}}(x)\to 0$ as $x\to\infty$. Now we have the following: No matter how $V^{\mathrm{small}}_{\mathrm{bar}}$ in (2.48) is chosen, we obtain in any case $\overline{\mathcal{T}}^{\epsilon}_{1\to 2}\neq 1/\,\mathbf{E}_{\bar{\mu}^{(1)}}[1/\mathcal{T}^{\epsilon}_{1\to 2}(x)]\to 0$. In this case we will have to incorporate the slow variable dynamics and use expected exit times (from a subset that will depend on the choice of $V^{\mathrm{small}}_{\mathrm{bar}}$) instead to derive the metastable transition times.

Situation 1: $V^{(1)}_{\mathrm{bar}}$ has a local minimum

Denote the minimum of $V^{(1)}_{\mathrm{bar}}$ by x_0, i.e., $V^{(1)}_{\mathrm{bar}}(x_0)=\min\{V^{(1)}_{\mathrm{bar}}(x):\,x\in\mathbf{R}\}$, and assume in addition $V^{(1)}_{\mathrm{bar}}$ tends to infinity as $|x|\to\infty$. Let $\bar{\mu}^{(1)}(x_0)$ be significantly larger than zero. By using Laplace's method, we get from (2.51) for small ς

$$\mathbf{E}_{\bar{\mu}^{(1)}}[1/\mathcal{T}^{\epsilon}_{1\to 2}(x)] \simeq$$
$$\sqrt{\frac{\omega^{(1)}(x_0)\omega_0(x_0)}{4\,\pi\,\partial_x^2 V^{(1)}_{\mathrm{bar}}(x_0)}}\;\frac{1}{Z^{(1)}}\;\exp(-\frac{2}{\sigma^2}V(x_0,m^{(1)}(x_0)))\;\frac{\varsigma}{\epsilon}\;\exp(-\frac{2}{\varsigma^2}V^{(1)}_{\mathrm{bar}}(x_0)),$$

where we have to assume that the second derivative of $V_{\rm bar}^{(1)}(x)$ wrt. x is non-null for $x = x_0$. By setting $V_{\rm bar}^{\rm small} = V_{\rm bar}^{(1)}(x_0)$ and coupling of ς to ϵ according to (2.48) we obtain $1/\,\mathbf{E}_{\bar\mu^{(1)}}[1/\mathcal{T}^{\epsilon}_{1\to 2}(x)] = \mathrm{ord}(1/\varsigma) \to \infty$. In this situation it is correct to set $\overline{\mathcal{T}}^{\epsilon}_{1\to 2} \simeq 1/\,\mathbf{E}_{\bar\mu^{(1)}}[1/\mathcal{T}^{\epsilon}_{1\to 2}(x)]$. The key point is that following Laplace we asymptotically have

$$\begin{aligned}
\overline{\mathcal{T}}^{\epsilon}_{1\to 2} &\simeq \left(\int_{D(\sigma)} 1/\mathcal{T}^{\epsilon}_{i\to j}(x)\,\bar\mu^{(i)}(x)\,\mathrm{d}x\right)^{-1} = \mathrm{ord}(\sqrt{\ln(1/\epsilon)}),\\
\varsigma(\epsilon) &= \left(\frac{2\,V_{\rm bar}^{(1)}(x_0)}{\ln(K/\epsilon)}\right)^{1/2}, \qquad K > 0,
\end{aligned}$$

for any connected region $D(\sigma)$ with the only assumption that x_0 is contained in the interior of $D(\sigma)$ and $\bar\mu^{(1)}(x_0)$ is larger than zero.

To determine the asymptotics of the metastable transitions times from $B^{(2)}$ to $B^{(1)}$, we assume for simplicity that $V_{\rm bar}^{(2)}$ satisfies the same properties as $V_{\rm bar}^{(1)}$, that is, there is one global minimum in the accessible x state space with $V_{\rm bar}^{(2)} \to \infty$ as $|x| \to \infty$. Without loss of generality we suppose $\min\{V_{\rm bar}^{(2)} : x \in \mathbf{R}\} = (1+\delta)V_{\rm bar}^{(1)}(x^0)$ for some $\delta > 0$. Then

$$\begin{aligned}
\overline{\mathcal{T}}^{\epsilon}_{2\to 1} &\simeq \mathrm{ord}(\epsilon^{-\delta}\sqrt{\ln(1/\epsilon)}),\\
\varsigma(\epsilon) &= \left(\frac{2\,V_{\rm bar}^{(1)}(x_0)}{\ln(K/\epsilon)}\right)^{1/2}, \qquad K > 0.
\end{aligned}$$

Situation 2: $V_{\rm bar}^{(1)}$ strictly monotonically decreasing to zero

For ease of presentation, we prefer to put the elaboration for this scenario in Appendix C.

2.2.6 OU-Averaged Dynamics and Conditional Averaging

To complete the discussion and re-establish the reference to the conditionally averaged system (1.21) we finally examine its closeness to the OU-averaged dynamics (2.47).

We basically have to compare the drift terms in (1.21) and (2.47) as well as the transition rate matrices. As outlined in Section 2.2.2, the transition rate matrix $\mathcal{Q}_x$ with entries given in (2.30) is (in the asymptotic limit $\varsigma \to 0$) equally well expressed as

$$\mathcal{Q}_x \simeq \frac{|\lambda_1(x)|}{\epsilon}\begin{pmatrix} -\mu_x(B_x^{(2)}) & \mu_x(B_x^{(2)}) \\ \mu_x(B_x^{(1)}) & -\mu_x(B_x^{(1)}) \end{pmatrix},$$

with $\lambda_1(x)$ denoting the first eigenvalue$\neq 0$ of the generator that corresponds to equation (2.29) for fixed x and $\epsilon = 1$. In this representation, the

matrix seems to be equal to $\mathcal{Q}_x$ as given in (1.18). However, there still is an obscurity concerning the metastable decomposition. According to (2.5), the metastable subsets that are used in (1.19) are given by the zero of the eigenfunction $u_1(x,\cdot)$ corresponding to $\lambda_1(x)$. It should be clear that the zero z must be somewhere between the two potential minima $m^{(1)}(x)$ and $m^{(2)}(x)$, but it is not clear that it asymptotically ($\varsigma \to 0$) approaches the saddle point $y_0(x)$. We come back to this problem below.

Let us assume for the moment that the zero z of u_1 approximates the saddle point in the limit $\varsigma \to 0$. We compare the drift terms in (1.21) and (2.47), which varies for fixed x in the probability density that is used to obtain the averaged force on the slow variable x. To this end, we apply standard Laplacian asymptotics in the limit of vanishing noise $\varsigma \to 0$. This provides us for $i = 1, 2$ with the precise estimates

$$\begin{aligned} \int D_x V(x,y)\, \mu_x^{\mathrm{OU}(i)}(y)\, \mathrm{d}y &\doteq D_x V(x, m^{(i)}(x)), \\ \int D_x V(x,y)\, \mu_x^{(i)}(y)\, \mathrm{d}y &\doteq D_x V(x, m^{(i)}(x)), \end{aligned}$$

which nicely shows that for decreasing ς the solution process of (2.47) comes arbitrarily close to the solution of the conditionally averaged system (1.21). Note that the derivative $D_x V(x, m^{(i)}(x))$ is taken wrt. the first component solely.

We shortly demonstrate that it is of considerable interest to have some knowledge about the zero of the eigenfunction u_1, as choosing an arbitrary point between the potential minima may lead to fatal approximation errors –not only for the transition rates but also for the drift term. To this end, consider the double-well potential $V(x,\cdot)$ (for fixed x) illustrated in Figure 2.6. We assume without loss of generality the shallow well to be at the left side, that is, $\min\{m^{(1)}(x), m^{(2)}(x)\} = m^{(2)}(x)$. Denote y_* the uniquely

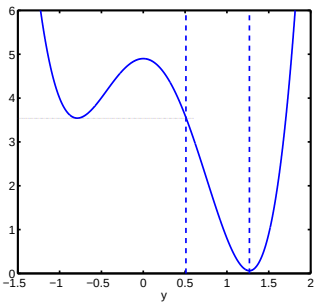

Figure 2.6: Asymmetric double-well potential. Any decomposition defined by a point z_* that is situated between the dashed lines leads to asymptotically wrong results if the decomposition is used for the conditionally averaged dynamics.

determined point $y_0(x) < y_* < m^{(2)}$ such that $V(x, y_*) = V(x, m^{(1)}(x))$,

and choose a point z_* with $y_* < z_* < m^{(2)}(x)$. The following considerations are based on the decomposition $\widehat{B}_x^{(1)} \cup \widehat{B}_x^{(2)}$ defined by

$$\widehat{B}_x^{(1)} \;=\; (-\infty, z_*) \qquad \widehat{B}_x^{(2)} \;=\; (z_*, \infty).$$

We again apply Laplace's method to obtain $\mu_x(\widehat{B}_x^{(1)})$ and $\mu_x(\widehat{B}_x^{(2)})$ in the asymptotic limit $\varsigma \to 0$:

$$\begin{aligned}
\mu_x(\widehat{B}_x^{(1)}) &= \frac{\int_{\widehat{B}_x^{(1)}} e^{-\frac{2}{\varsigma^2}V(x,y)}\mathrm{d}y}{\int e^{-\frac{2}{\varsigma^2}V(x,y)}\mathrm{d}y} \doteq \frac{2\varsigma\omega^{(2)}(x)}{D_yV(x,z_*)}\, e^{-\frac{2}{\varsigma^2}\left(V(x,z_*)-V(x,m^{(2)}(x))\right)}, \\
\mu_x(\widehat{B}_x^{(2)}) &= \frac{\int_{\widehat{B}_x^{(2)}} e^{-\frac{2}{\varsigma^2}V(x,y)}\mathrm{d}y}{\int e^{-\frac{2}{\varsigma^2}V(x,y)}\mathrm{d}y} \doteq 1,
\end{aligned}$$

and, consequently, comparison to the metastable subsets defined by the saddle point, yields

$$\mu_x(B_x^{(1)}) \ll \mu_x(\widehat{B}_x^{(1)}), \qquad \mu_x(B_x^{(2)}) \simeq \mu_x(\widehat{B}_x^{(2)}).$$

Therefore, assuming $z \approx z_*$ for the zero of u_1 would result in asymptotically larger transition rates $|\lambda_1^\epsilon(x)|\mu_x(\widehat{B}_x^{(1)})$ ($\lambda_1^\epsilon = \lambda_1/\epsilon$) from the deep to the shallow well in comparison to the rates as given in (2.30). For the drift terms this would imply for fixed x

$$\begin{aligned}
\int_{\widehat{B}_x^{(2)}} D_xV(x,y)\,\mu_x(y)\,\mathrm{d}y &\doteq D_xV(x,m^{(2)}(x)), \\
\int_{\widehat{B}_x^{(1)}} D_xV(x,y)\,\mu_x(y)\,\mathrm{d}y &\doteq D_xV(x,z_*(x)),
\end{aligned}$$

which obviously is not asymptotically equal to the drift term in (2.47) for $i = 1$.

Asymptotics of Second Eigenfunction

We now demonstrate that the zero z of the second eigenvector $u_1(x,\cdot)$ approximates the saddle point $y_0(x)$ in the asymptotic limit $\varsigma \to 0$.

For the derivation of $u_1(x,\cdot)$ we follow the line of Pavlyukevich in [36]. He suggested to look for the solution of $\mathcal{L}_x u_1(x,y) = \lambda_1(x)\, u_1(x,y)$ in form of a power series in the parameter $\lambda_1(x)$, formally

$$u_1(x,y) \;=\; u_1^{(0)}(x,y) \;+\; \lambda_1(x)u_1^{(1)}(x,y) \;+\; (\lambda_1(x))^2u_1^{(2)}(x,y) \;+\; .... \quad (2.52)$$

Substituting (2.52) into the eigenvalue equation induces ordinary differential equations for $u_1^{(k)}$. More precisely, $u_1^{(0)}$ satisfies the homogeneous equation

$$\frac{\sigma^2}{2}\Delta_y u_1^{(0)}(x,y) \;-\; D_yV(x,\cdot)\, D_y u_1^{(0)}(x,y) \;=\; 0, \quad x \in \mathbf{R}^m,\, y \in \mathbf{R}, \quad (2.53)$$

whereas for $k \geq 1$

$$\frac{\sigma^2}{2}\Delta_y u_1^{(k)}(x,y) - D_y V(x,\cdot)\, D_y u_1^{(k)}(x,y) = u_1^{(k-1)}(x,y),\ x \in \mathbf{R}^m, y \in \mathbf{R}.$$

The results of the above equations are explicitly computed in [36]. For the zeroth order approximation we obtain

$$\begin{aligned} u_1^{(0)}(x,\cdot) &= h_0(x,\cdot)\mathbf{1}_{(-\infty,m^{(1)}(x)]}(y) \\ &+ f_0(x,\cdot)\mathbf{1}_{[m^{(1)}(x),m^{(2)}(x)]}(y) + g_0(x,\cdot)\mathbf{1}_{[m^{(2)}(x),\infty)}(y), \end{aligned} \quad (2.54)$$

where the functions h_0, f_0 and g_0 are defined by

$$\begin{aligned} h_0(x,y) &= a, \qquad x \in \mathbf{R}^m,\ y \in (-\infty, m^{(1)}(x)], \\ f_0(x,y) &= a + (b-a)\,\frac{\int_{m^{(1)}(x)}^{y} e^{\frac{2}{\varsigma^2}V(x,\tilde{y})}\mathrm{d}\tilde{y}}{\int_{m^{(1)}(x)}^{m^{(2)}(x)} e^{\frac{2}{\varsigma^2}V(x,\tilde{y})}\mathrm{d}\tilde{y}}, \\ &\qquad x \in \mathbf{R}^m,\ y \in [m^{(1)}(x), m^{(2)}(x)], \\ g_0(x,y) &= b, \qquad x \in \mathbf{R}^m,\ y \in [m^{(2)}(x), \infty), \end{aligned}$$

where a, $b \in \mathbf{R}$ have to be determined in the small noise limit $\varsigma \to 0$ such that $\langle u_1, \mathbf{1}\rangle_{\mu_x} = 0$ and $u_1(x,\cdot) \in L^2(\mu_x)$. To simplify notation, we desist from normalizing the function $u_1(x,\cdot)$, simply put $a = 1$ and look for b. Pavlyukevich presents in [36, Chapter 5.4] the constant b as a function of ς according to

$$b = -\frac{\omega^{(2)}(x)}{\omega^{(1)}(x)} \exp\Big(-\frac{2}{\varsigma^2}\big(V(x,m^{(1)}) - V(x,m^{(2)}(x))\big)\Big)\,(1 + \mathcal{O}(\varsigma^2)).$$

Note, that $V(x,m^{(1)}(x)) - V(x,m^{(2)}(x)) = V_{\mathrm{bar}}^{(2)}(x) - V_{\mathrm{bar}}^{(1)}(x)$. Now, we easily observe pointwise convergence for every x and y

$$\begin{aligned} \lim_{\varsigma\to 0} f_0(x,y) &= a > 0, \qquad y \in (-\infty, y_0(x)), \\ \lim_{\varsigma\to 0} f_0(x,y) &= b < 0, \qquad y \in (y_0(x), \infty), \end{aligned}$$

and, together with the result (from [36])

$$\max_{y\in\mathbf{R}} |u_1(x,\cdot) - u_1^{(0)}(x,\cdot)| \doteq 0$$

from [36], we conclude that the zero $z = z(x)$ of the eigenfunction $u_1(x,\cdot)$ is asymptotically given by the saddle point, that is, $z(x) = y_0(x)$ in the limit $\varsigma \to 0$.

Note that $u_1^{(0)}(x,\cdot)$ is not contained in the domain of $\mathcal{L}_x$, cf. Remark 3.5.3.

2.3 Numerical Experiments

In this section we illustrate the results from the preceding section by numerical experiments with an appropriate test example.

2.3.1 Design of Appropriate Test System

We consider the Smoluchowski equation

$$\dot{x}^\epsilon = -D_x V(x,y) + \sigma \dot{W}_1 \tag{2.55}$$

$$\dot{y}^\epsilon = -\frac{1}{\epsilon} D_y V(x,y) + \frac{\varsigma}{\sqrt{\epsilon}} \dot{W}_2, \tag{2.56}$$

where the potential for the numerical analysis is given by:

$$V(x,y) = 2.5 \cdot (y^2-1)^2 - 0.8\, x\, y^3 + 0.005\, x^4 + 1.6, \tag{2.57}$$

which clearly satisfies Assumption 2.2.1. The potential energy surface is shown in Figure 2.7. At the left hand side of Figure 2.8 we illustrate the

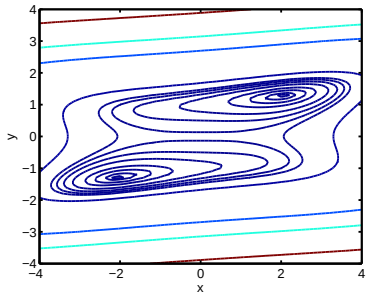

Figure 2.7: Full potential V.

double-well potentials $V(x,\cdot)$ for different values of x. The saddle point always is $y_0(x) = 0$ and takes the value $V(x,0) = 4.1 + 0.005\, x^4$, the potential minima are

$$m^{(i)}(x) = 0.12\, x + (-1)^i \sqrt{0.0576\, x^2 + 4}, \qquad i = 1, 2.$$

The right side of Figure 2.8 shows the potential barriers $V^{(1)}_{\text{bar}}(x)$ (the left barrier) and $V^{(2)}_{\text{bar}}(x)$ (the right barrier) as functions of x.

In Fig. 2.9 we show a typical realization of the dynamics (2.55)&(2.56) with $\sigma = 1.0$, $\varsigma = 0.75$ and $\epsilon = 0.0064$. For the generation of the trajectories we use the Euler-Maruyama scheme with internal time step $\mathrm{d}t = \epsilon/100$. We clearly observe that jumps between the metastable decomposition $B^{(1)} = \{(x,y) \,|\, y < 0\}$ and $B^{(2)} = \{(x,y) \,|\, y > 0\}$ induce metastable transitions in the x dynamics between $x < 0$ and $x > 0$. Comparison with the averaged

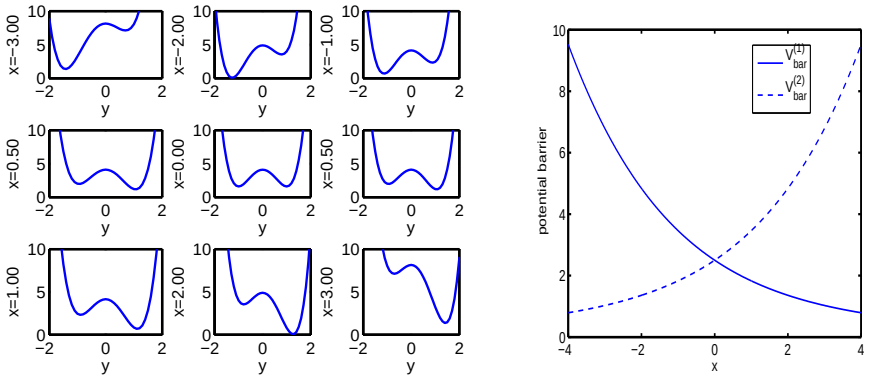

Figure 2.8: Left: Potentials $V(x,\cdot)$ in y for different values of x. Right: potential barriers $V^{(1)}_{\text{bar}}(x)$ (full line) and $V^{(2)}_{\text{bar}}(x)$ (dashed line).

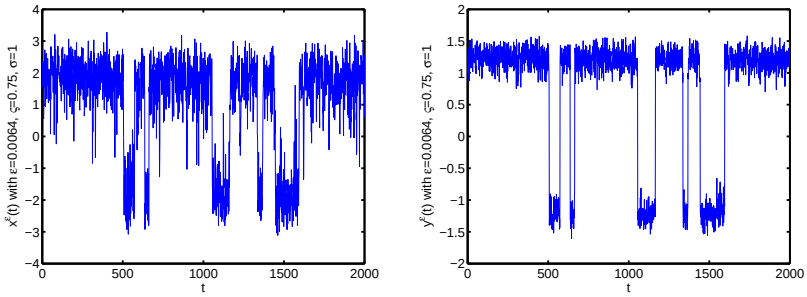

Figure 2.9: Typical realization of the original dynamics for $\sigma = 1.0$, $\varsigma = 0.75$ and $\epsilon = 0.0064$. Left: trajectories x cooridnate; right: trajectories y coordinate.

trajectory in Fig. 2.10 reveals inappropriateness of the standard averaging procedure (1.8). In Fig. 2.10 right we illustrate the averaged potential $\overline{V}$ that is associated with the realization at the left:

$$\overline{V}(\varsigma, x) \;=\; -\frac{\varsigma^2}{2} \ln \int \exp\Big(-\frac{2}{\varsigma^2} V(x,y) \Big)\, \mathrm{d}y.$$

Using standard Laplace asymptotics provides us with the potential in the limit $\varsigma \to 0$ of vanishing fast diffusion

$$\overline{V}(x) \;=\; \min\{V\big(x, m^{(1)}(x)\big), V\big(x, m^{(2)}(x)\big)\}.$$

In Fig. 2.10 we additionally plotted $\overline{V}(x)$, which graphically is completely identical to $\overline{V}(\varsigma = 0.75, x)$.

Fig. 2.9 & 2.10 explicitly visualize the simply averaged dynamics to be inappropriate to describe the effective dynamical behaviour of $x^\epsilon(t)$ as $\epsilon \to 0$. For small ϵ diffusion in y is very fast compared to diffusion in x. However, the important (and only) barriers of the potential are barriers in y

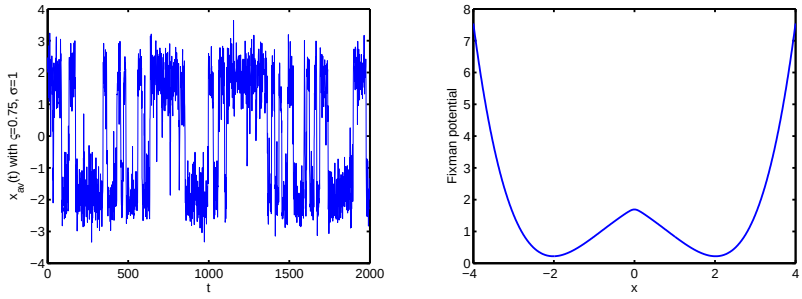

Figure 2.10: Left: Typical realization of the simply averaged dynamics (1.8) for $\sigma = 1.0$, $\varsigma = 0.75$. Right: Fixman potential that corresponds to the trajectory at the left.

direction. Thus, for fixed ϵ, decreasing the noise intensity ς in the fast equation increases the metastability in y. Consequently, by choosing different ς one can analyze the effect of increasing metastability on averaging. To this end, it is convenient to use the x averaged values of the expected transition rates $1/\mathcal{T}^{\epsilon}_{i\to j}(x)$. As detailed in Section 2.2.5 this provides us in the asymptotic limit $\varsigma \to 0$ with the expected transition times $\overline{\mathcal{T}}^{\epsilon}_{1\to 2}$ between the metastable decomposition $B^{(1)} \cup B^{(2)}$ in the (x, y) state space. We generated $N = 2000$ realizations of the original dynamics[12] for $\epsilon = 0.0064$, $\sigma = 1.0$ and $\varsigma = 0.75, 0.7, 0.65, 0.60$, and waited for the first exit times from $B^{(1)}$. Fig. 2.11 at the top illustrates the location of the trajectories x-coordinate right before the transitions occurred; the pictures at the bottom display the function under the integral in (2.51) (normalized to 1) and nicely illustrate that the major contribution to the integral in (2.51) will move rightwards as $\varsigma \to 0$, for $V^{(1)}_{\mathrm{bar}}(x) \to 0$ as $x \to \infty$. Comparison of the upper and the lower pictures reveals almost coincidence between the contribution to the integral in (2.51) and the actual location in the x space of the jumps from $B^{(1)}$ to $B^{(2)}$. Finally, we compare in Table 2.4 the averaged values of the transition times (they are calculated by means of 2.49) to the numerically obtained values by means of the $N = 2000$ realizations. We observe that ς has to be chosen small to get closeness.

Discretization

The pathwise simulation of the dynamics consisting of the two state Markov jump process $I(t, x)$ is developed by using a specific stochastic particle method ([18]). To this end, recall the infinitesimal generator $\mathcal{Q}^{\epsilon}_x = (q^{\epsilon}_{ij}(x))_{i,j=1,2}$ that allows to calculate the hopping probabilities between the states $\mathbf{S} =$

[12] Actually, we have not used the original dynamics (2.55)&(2.56), for it is not possible to compute the realizations within a reasonable period of time. Instead we used the conditionally averaged system (1.21) with $I(t, x) = 1$ and computed the transition time to $I(t, x) = 2$. According to the considerations in Subsection 2.3.2 this yields perfect coincidence with the original dynamics' transitions from $B^{(1)}$ to $B^{(2)}$.

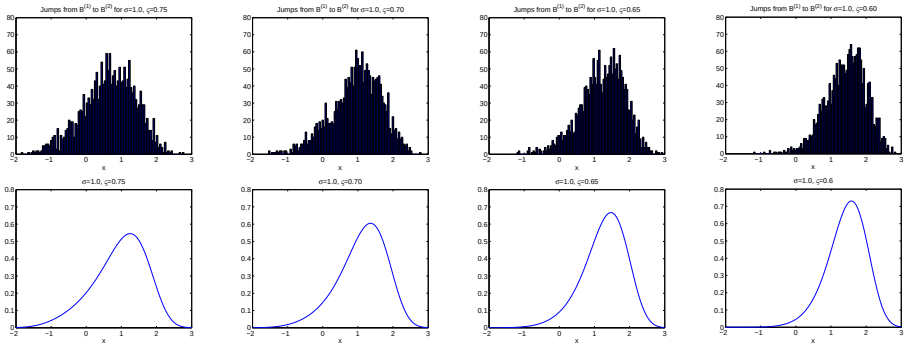

Figure 2.11: Top: Transition location (from $B^{(1)}$ to $B^{(2)}$) of the trajectories x-coordinate computed by means of $N = 2000$ realizations of the conditionally averaged dynamics for $\sigma = 1.0$, $\epsilon = 0.0064$ fixed and $\varsigma = 0.75, 0.7, 0.65, 0.6$. Bottom: Function under the integral in (2.51) normalized to 1 by using the same parameters as above.

Mean transition times	$\varsigma = 0.75$	$\varsigma = 0.7$	$\varsigma = 0.65$	$\varsigma = 0.60$
mean value from 2000 real.	213	462	1240	4285
averaged value $\overline{\mathcal{T}}^{\epsilon}_{1\to 2}$	119	323	1037	4157

Table 2.4: Expectation values of transition times from $B^{(1)}$ to $B^{(2)}$ corresponding to Fig. 2.11.

$\{1, 2\}$. The transition matrix $P^{\epsilon}_{\tau}(x) = (p^{\epsilon}_{ij}(\tau, x))$ at time τ is then obtained by

$$P^{\epsilon}_{\tau}(x) \;=\; \exp(\tau \mathcal{Q}^{\epsilon}_{x}).$$

A straightforward calculation reveals

$$\begin{aligned} p^{\epsilon}_{12}(\tau, x) &= \frac{q^{\epsilon}_{12}(x)}{q^{\epsilon}_{12}(x) + q^{\epsilon}_{21}(x)} \left(1 - e^{-\tau(q^{\epsilon}_{12}(x) + q^{\epsilon}_{21}(x))}\right), \\ p^{\epsilon}_{21}(\tau, x) &= \frac{q^{\epsilon}_{21}(x)}{q^{\epsilon}_{12}(x) + q^{\epsilon}_{21}(x)} \left(1 - e^{-\tau(q^{\epsilon}_{12}(x) + q^{\epsilon}_{21}(x))}\right). \end{aligned}$$

The entries of $\mathcal{Q}^{\epsilon}_{x}$ are given in (2.30) by the inverse of the precise estimates of the expected transition times over the potential energy barrier in y direction.

The stochastic particle method requires two steps. We shortly demonstrate it for the OU-averaged dynamics (2.47).

Step 1: Transport. The first step consists of determining an updated position $x(t + \mathrm{d}t)$ by solving

$$\dot{x} \;=\; -\int D_x V(x, y) \cdot \mu^{\mathrm{OU}(i)}_{x}(y)\, \mathrm{d}y \;+\; \sigma \dot{W}_1,$$

over $[0, \mathrm{d}t]$ with initial point $x(t)$.

Step 2: Exchange. The second step models the exchange between the states $I(t,x) = 1$ and $I(t,x) = 2$. Thus, if $i = 1$, we set $i = 2$ with hopping probability $p_{1\to 2} = p^{\epsilon}_{12}(\mathrm{d}t, x(t+\mathrm{d}t))$ and remain at $i = 1$ with probability $1 - p_{1\to 2}$. Vice versa, if $i = 2$, we set $i = 1$ with hopping probability $p_{2\to 1} = p^{\epsilon}_{21}(\mathrm{d}t, x(t+\mathrm{d}t))$ and remain at $i = 2$ with probability $1 - p_{2\to 1}$. Return to step 1 by setting $x(t) = x(t+\mathrm{d}t)$.

Parameter Choice

Subsequently, we choose the noise intensity in the slow equation to be $\sigma = 1$, and the smallness parameter is set to $\epsilon = 0.0064$. Trajectories are illustrated with $\varsigma = 0.75$, whereas comparison of exit times suggests to use different values of ς.

Recalling the coupling of ς to ϵ according to (2.48), some words seem to be necessary concerning the comparison of the full dynamics to the OU-approximated ones: Without loss of generality we can choose ς arbitrary without considering the coupling, for the experiments are performed for a fixed value of ϵ. Therefore, for fixed $\epsilon = \epsilon^*$ and fixed $\varsigma = \varsigma^*$ we can always find a constant $K = K^*$ (or a barrier $V^{\mathrm{small}}_{\mathrm{bar}} = V^{\mathrm{small}*}_{\mathrm{bar}}$) such that $\varsigma(\epsilon^*) = \varsigma^*$ under (2.48). Even if we take (2.33) as the basis of our computation, we can desist from the coupling rule, for the constant K then can be chosen dependent of x, such that we still arrive at $\varsigma(\epsilon^*, x) = \varsigma^*$. Actually, the postulation of relating ς to ϵ only serves as a formal justification of the OU approximation. For the numerical implementation only the size of ς by its own is of importance, not its relation to ϵ.

The motivation to choose $\sigma = 1.0$ and not $\sigma = \varsigma$ can be inferred from Fig. 2.11. In case of smaller values of σ, say $\sigma = 0.75$, the x-coordinate of the trajectory will hardly reach the region where the jumps mostly happen. Then we had to choose ς larger, which on its part would result in a worse OU approximation[13].

2.3.2 Comparison Between Original Dynamics and Dynamics with Fast OU Processes

Here, we carry out numerical studies in order to compare the Smoluchowski dynamics (2.28)&(2.29) with those governed by system (2.31)&(2.32) with fast OU processes and transition chain $I(t,x)$ that controls the switches between the two OU processes.

Typical realizations of both the original dynamics and the OU approximated dynamics (2.31)&(2.32) are shown in Figure 2.12. The trajectories have been generated using the Euler-Maryuana scheme with time step $\mathrm{d}t = \epsilon/100$ for both systems. Apparently, the transition rates between $B^{(1)}$

[13]For small σ it is not possible to numerically compute the expected exit times within a reasonable period of time.

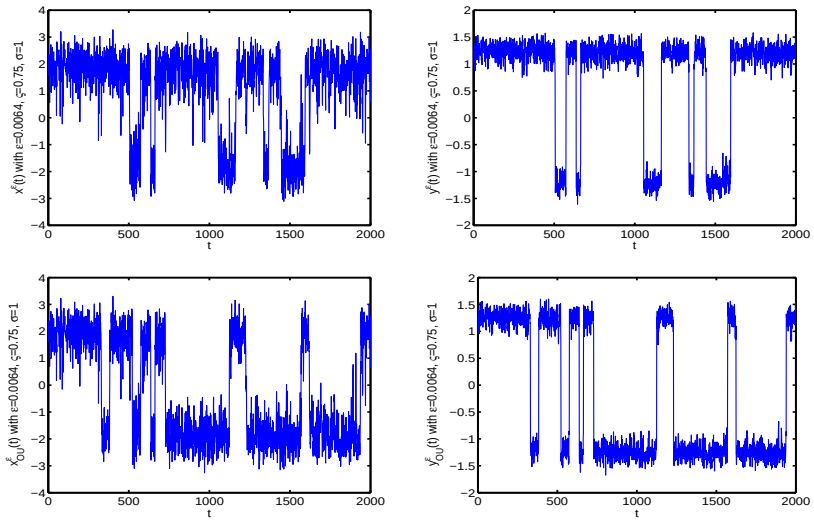

Figure 2.12: Typical realization of the original dynamics (top) and the approximated dynamics with fast OU processes (bottom). At the left we see the x, at the right the y coordinate. The realizations have been computed for the same realization of the white noise (in the slow and in the fast equation).

and $B^{(2)}$ coincide to some extend and the oscillating motion (around the potential minima in y) inbetween the transitions seems to be well approximated by using OU processes in the fast equation. We clearly observe that jumps induce metastable transitions in the x dynamics between $x < 0$ and $x > 0$. However, for the trajectories being in $B^{(1)}$ we observe the x-coordinate of the original dynamics to spread considerably further rightwards than the x trajectory of the approximated system (and for the trajectories in $B^{(2)}$ the original dynamics' x-coordinate spreads further leftwards).

The above consideration concerning the x trajectories' behaviour suggests that the original dynamics have noticeable smaller transition times between $B^{(1)}$ and $B^{(2)}$, for the original dynamics more often reaches a domain where the potential barriers (in y direction) are small. This is confirmed by Table 2.5, where we computed the expected transition times from $B^{(1)}$ to $B^{(2)}$ by means of $N = 2000$ realizations for different values of ς and $\sigma = 1.0$, $\epsilon = 0.0064$ fixed. We come back to this problem in the next section

dynamical model	$\varsigma = 0.8$	$\varsigma = 0.75$
original dynamics	113	210
dynamics with OU process	136	265

Table 2.5: Exit times from the set $B^{(1)}$ for the original dynamics and the OU-approximated system.

where we include the averaged dynamics into our numerical considerations. Actually, it will turn out that ς has to be chosen very small to get perfect coincidence of both the original and the approximated (full) system.

2.3.3 Results Including Averaged Dynamics

We now demonstrate pre-eminence of the OU-averaged dynamics (2.47). To complete the representation we include the conditionally averaged dynamics (1.21).

In Figure 2.13 we compare realizations of the averaged to the full dynamics' x-coordinate. Every trajectory has been computed with the same realization of white noise $\dot{W}_1$, $\dot{W}_2$, such that the internal time step has been set to $\mathrm{d}t = \epsilon/100$ even for the averaged dynamics. The Markov jump process $I(t, x)$ is realized by using one realization of random numbers for every concerned system. Concerning the systems with OU processes (full and OU-

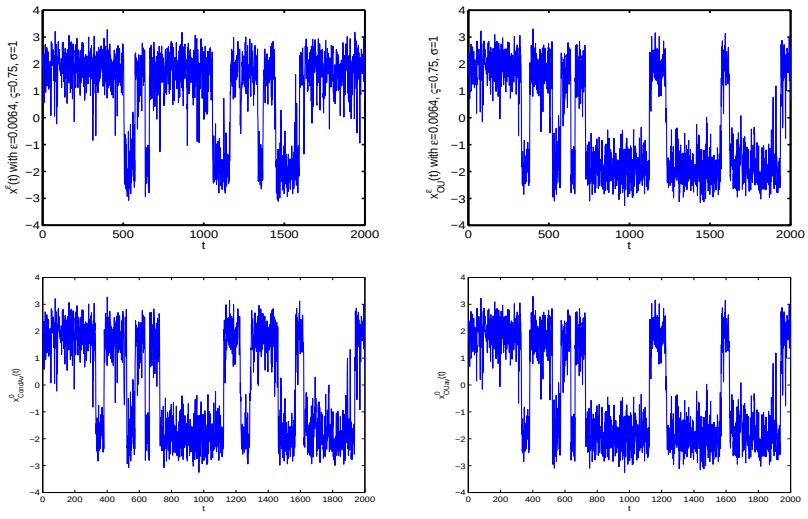

Figure 2.13: Realizations of the original dynamics x coordinate (top, left), the x coordinate of the full OU-approximated system (top, right), the OU-averaged (bottom, right), and the conditionally averaged system (bottom, left).

averaged), we observe pathwise convergence of the x trajectories, whereas comparison of the original dynamics with the conditionally averaged system reveals distributional coincidence.

In order to present numbers instead of pictures we want to compute the expectation values of the metastable transition times from $x < 0$ to $x > 0$ for different values of ς. It is natural to expect that this is realized by computing the first exit times from the set $S + \delta$ with $S = \{x \in \mathbf{R} \,|\, x < 0\}$, where $\delta > 0$ has to be large enough to guarantee that the process effectively reaches some (small) region of attraction in the complement of S. But Fig. 2.11

nicely shows that the x-coordinate of the original dynamics (respectively the conditionally averaged dynamics) can spread far into the positive region even when it is restricted to the metastable set S. Thus, we suggest to define the stopping time as the first exit from $B^{(1)}$ instead, respectively the first jump from $I(t,x) = 1$ to $I(t,x) = 2$. At least for $\varsigma \leq 7.5$ (compare Fig. 2.12) this is equivalent to the metastable transitions from $x < 0$ to $x > 0$. From $N = 2000$ realizations for $\epsilon = 0.0064$ and $\sigma = 1.0$ we get

dynamical model	$\varsigma = 0.8$	$\varsigma = 0.75$	$\varsigma = 0.65$
original dynamics	113	210	$--$
cond. averaged dyn.	105	213	1240
OU-approx.full dyn.	136	265	$--$
OU-averaged dyn.	135	265	1537

Table 2.6: Comparison of exit times from the metastable set $S = \{x \in \mathbf{R} \mid x < 0\}$. For $\varsigma = 0.65$, it was not possible to compute the exit times of the full dynamics' motion within a reasonable period of time.

a very good agreement between the OU-approximated dynamics and the OU-averaged dynamics, and a good agreement between the original and the conditionally averaged dynamics.

However, there still remains the problem of diversity between the OU-averaged and the conditionally averaged dynamics. To overcome the problem, we illustrate in Fig. 2.14 the potentials that correspond to the respective trajectories for $\varsigma = 0.75, 0.60, 0.3$. For $I(t,x) = i \in \{1,2\}$ and ς fixed, the

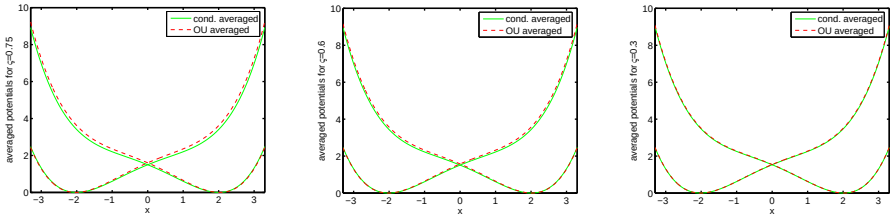

Figure 2.14: Comparison of conditionally averaged (full line) to OU-averaged potentials (dashed line).

conditionally averaged potential $\overline{V}^{(i)}(\varsigma, x)$ and the OU-averaged potential $\overline{V}^{\mathrm{OU}(i)}(\varsigma, x)$ are defined implicitly by

$$\begin{aligned} D_x \overline{V}^{\mathrm{OU}(i)}(\varsigma, x) &= \int D_x V(x,y)\, \mu_x^{\mathrm{OU}(i)}(y)\, \mathrm{d}y, \\ D_x \overline{V}^{(i)}(\varsigma, x) &= \int D_x V(x,y)\, \mu_x^{(i)}(y)\, \mathrm{d}y, \end{aligned}$$

and we easily show that

$$\overline{V}^{(i)}(\varsigma, x) \;=\; -\frac{\varsigma^2}{2} \ln \int_{B_x^{(i)}} \exp\big(-\frac{2}{\varsigma^2} V(x,y)\big)\, \mathrm{d}y.$$

Exploiting the estimation method of Laplace we obtain asymptotical identity of both potentials:

$$\lim_{\varsigma \to 0} \overline{V}^{(i)}(\varsigma, x) \;=\; \lim_{\varsigma \to 0} \overline{V}^{\mathrm{OU}(i)}(\varsigma, x) \;=\; V(x, m^{(i)}(x)).$$

Fig. 2.14 reveals $\overline{V}^{(i)}(\varsigma, x) \approx \overline{V}^{\mathrm{OU}(i)}(\varsigma, x)$ for $\varsigma \leq 0.3$, whereas they differ visibly for $\varsigma \geq 0.60$ in that region where the jumps from $i = 1$ to $i = 2$ mostly happen. This perfectly explains the significant difference concerning the transition times in Tables 2.5 & 2.6.